# Diagenesis and Burial History of Nonmarine Upper Cretaceous Rocks in the Central Uinta Basin, Utah

U.S. GEOLOGICAL SURVEY BULLETIN 1787–D

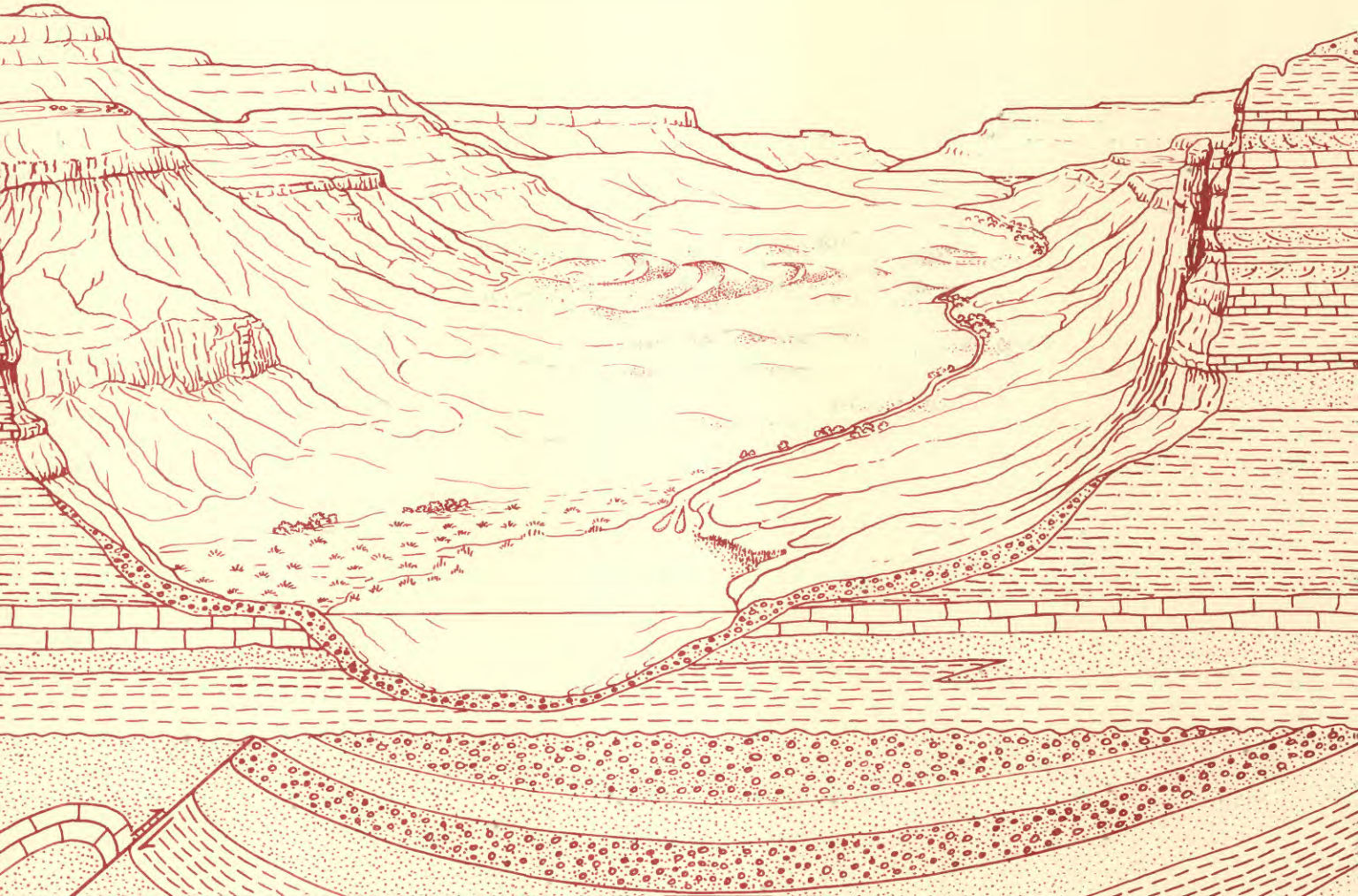

Chapter D

# Diagenesis and Burial History of Nonmarine Upper Cretaceous Rocks in the Central Uinta Basin, Utah

By JANET K. PITMAN, KAREN J. FRANCZYK, and DONALD E. ANDERS

A multidisciplinary approach to research studies of
sedimentary rocks and their constituents and
the evolution of sedimentary basins, both ancient and modern

U.S. GEOLOGICAL SURVEY BULLETIN 1787

EVOLUTION OF SEDIMENTARY BASINS—UINTA AND PICEANCE BASINS

DEPARTMENT OF THE INTERIOR
DONALD PAUL HODEL, Secretary

U.S. GEOLOGICAL SURVEY
Dallas L. Peck, Director

UNITED STATES GOVERNMENT PRINTING OFFICE, WASHINGTON: 1988

For sale by the
Books and Open-File Reports Section
U.S. Geological Survey
Federal Center
Box 25425
Denver, CO 80225

**Library of Congress Cataloging-in-Publication Data**
(Revised for Ch. D)

Evolution of sedimentary basins—Uinta and Piceance basins.

(U.S. Geological Survey bulletin ; 1787 A– )
Includes bibliographies.
Supt. of Docs. no.: I 19.3:1787–D
Contents: ch. A. Sedimentology and paleographic significance of six fluvial sandstone bodies in the Maroon Formation, Eagle Basin, northwest Colorado / by Samuel Y. Johnson. ch. B. Sedimentology of an eolian sandstone from the Middle Pennsylvanian Eagle Valley Evaporite, Eagle Basin, northwest Colorado / by Christopher J. Schenk. -- [etc.] -- ch. D. Diagenesis and burial history of nonmarine Upper Cretaceous rocks in the central Uinta basin, Utah / by Janet K. Pitman, Karen J. Franczyk, and Donald E. Anders.
1. Sedimentation and deposition. 2. Geology—West (U.S.) I. Johnson, Samuel Y. II. Schenk, Christopher J. III. Nuccio, Vito F. IV. Series.
QE75.B9 no. 1787 A–C 557.3 s [551.3] 87-27737
[QE571]

# CONTENTS



FIGURES

TABLES

# Diagenesis and Burial History of Nonmarine Upper Cretaceous Rocks in the Central Uinta Basin, Utah

*By* Janet K. Pitman, Karen J. Franczyk, *and* Donald E. Anders

**Abstract**

Rocks of the Upper Cretaceous nonmarine undifferentiated Tuscher and Farrer Formations in the Uinta basin of northeast Utah yield thermogenic gas and some oil from carbonaceous shales and coal beds. These rocks, interbedded with fine-grained, lenticular, low-permeability sandstones, formed in a complex meandering and locally braided fluvial system in the Cretaceous Western Interior foreland basin.

Reservoir sandstones in the lowest cored sequence comprise quartz arenites and sublitharenites that are compositionally and diagenetically similar to rocks of the underlying Neslen Formation. Feldspathic sandstones in the upper cored sequence have a more complex diagenetic history than previously reported for either the Tuscher or Farrer Formations, a history that includes development of early quartz overgrowths and precipitation of iron chlorite rim cement, followed by dissolution of nonferroan and ferroan carbonate, crystallization of illite and chlorite in secondary pores, and finally localized formation of anhydrite and barite cement. Stable isotope studies indicate that isotopically heavy nonferroan carbonate formed early, at relatively shallow burial depths. Isotopically lighter ferroan carbonate, which reflects diagenetic modification at greater depths of burial and higher temperatures, is associated with bitumen and anhydrite. Porosity and permeability in rocks of the Tuscher and Farrer Formations typically are low. Porosity is reduced wherever deformed lithic grains, matrix, and authigenic clay are abundant and is enhanced wherever dissolution of carbonate and sulfate minerals and feldspar or chert grains has occurred.

Geochemical studies indicate that gas-prone source rocks in the Tuscher and Farrer Formations in the central Uinta basin are within the zone of catagenesis. A modified time–temperature Lopatin burial history model indicates that active hydrocarbon generation began about 30 Ma, when the rocks reached their maximum burial depth and temperature and following deposition of approximately 9,000 ft (2,743 m) of Tertiary sediments during basin subsidence. The similarity between past and present-day geothermal gradients (1.6 °F/100 ft; 29 °C/km) in the Wilkin Ridge well suggests that heat flow through the central part of the basin has been relatively uniform from the Late Cretaceous to the present.

## INTRODUCTION

The Upper Cretaceous, nonmarine, undifferentiated Tuscher and Farrer Formations in the Uinta basin of northeastern Utah locally contain thermogenic gas that was generated in place from carbonaceous shales and discrete coal beds. These gas-bearing rocks are complexly interbedded with lenticular, diagenetically modified, low-permeability sandstones. Successful exploration in these units has been difficult because of complex patterns of sandstone distribution, thickness, and geometry and variations in reservoir quality resulting from postdepositional mineral alteration. Moreover, source rock potential in the Tuscher and Farrer Formations throughout the basin is poorly understood because little is known about their hydrocarbon generation history.

Three cores of the undifferentiated Tuscher and Farrer Formations were taken in the Exxon No. 1 Wilkin Ridge well in the central Uinta basin (sec. 29, T. 10 S., R. 17 E.; fig. 1). Based on geophysical log responses, the Tuscher and Farrer Formations can be divided into a lower unit, represented by the cored interval from 11,185 to 11,230 ft (3,409–3,423 m), and an upper unit, which includes cores from two intervals, 10,740 to 10,803 ft (3,274–3,293 m) and 10,273 to 10,295 ft (3,131–3,138 m). These cores represent the most deeply buried rocks of the Tuscher and Farrer Formations that are available for study and can be compared with less deeply buried, temporally equivalent units in other parts of the basin.

Distinct, commonly abrupt compositional changes in mineralogy from dominantly quartz to increasing amounts of feldspar have been observed between the Bluecastle Tongue of the Castlegate Sandstone and the overlying Tuscher and Farrer Formations in the southern, western, and central parts of the Uinta basin (Keighin and Fouch, 1981; Lawton, 1983; Pitman, Anders, and others, 1986). Our studies of the Wilkin Ridge well indicate that rocks of the Tuscher and Farter Formations are mineralogically complex, in that they contain a quartzose

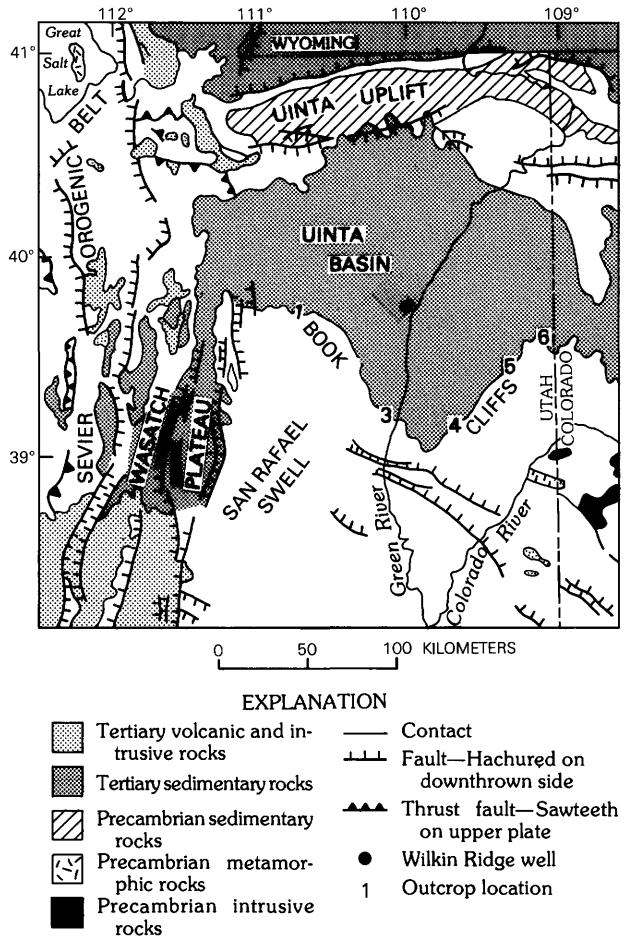


**Figure 1.** Location of Wilkin Ridge well and selected orogenic features and rock types, Uinta basin, northeast Utah.

mineral facies typical of the older Neslen Formation as well as a lithofeldspathic facies that is characteristic of these formations in other areas of the basin. Local variations in framework composition are accompanied by varied diagenetic patterns that reflect differing physiochemical conditions during burial. Time-temperature models indicate that intense hydrocarbon generation occurred in the central part of the Uinta basin during the early Oligocene, at which time potential source rocks in the Tuscher and Farrer Formations reached their maximum burial depth and paleotemperature. The results of our study should be useful in recognizing diverse mineral facies distributions within the Tuscher and Farrer Formations and in future exploration and evaluation of these complex hydrocarbon source and reservoir rocks.

*Acknowledgments.*—We thank Exxon Oil Company for providing core material and production data for the Wilkin Ridge well. We are also grateful to T.D. Fouch, U.S. Geological Survey, who described the core and engaged in numerous stimulating discussions on Uinta basin geology. Global Geochemistry Corporation determined carbon and oxygen isotope contents, and Mark Pawlewicz, U.S. Geological Survey, performed vitrinite reflectance analyses. W.B. Cashion and C.J. Schenk, U.S. Geological Survey, provided helpful comments to improve this manuscript. Our research was supported by the U.S. Geological Survey Evolution of Sedimentary Basins Program.

## GEOLOGIC SETTING

Significant stratigraphic, nomenclature, facies, and thickness changes characterize Cretaceous rocks in the central Uinta basin. The area of the Wilkin Ridge well marks the transition from rapid tectonic subsidence near the Sevier thrust belt in the western part of the basin to a more tectonically stable area in the eastern part (fig. 1). Figure 2 shows a schematic chronostratigraphic cross section of Cretaceous and lower Tertiary rocks from the Book Cliffs near Price, Utah, to the Colorado-Utah State line. The projected outcrop equivalent of the Upper Cretaceous section in the Wilkin Ridge well is between the Sunnyside and Green River locations (figs. 1, 2), and, although analogies can be drawn between the outcrop and subsurface section, local differences probably exist in depositional events, subsidence rates, and effects of Late Cretaceous uplift and erosion. Comparison of depositional environments inferred from core and well logs of the Wilkin Ridge well to those ascertained from outcrop studies along the Book Cliffs helps delineate regional changes in facies patterns and burial history important in understanding and predicting distribution, abundance, and thermal evolution of hydrocarbon source and reservoir rocks.

Cretaceous rocks from the Wilkin Ridge well include (from oldest to youngest) 260 ft (79 m) of the uppermost, coal-bearing, nonmarine part of the Blackhawk Formation; 600 ft (183 m) of the nonmarine Castlegate Sandstone, which can be subdivided into three members; and about 2,000 ft (610 m) of the nonmarine, undifferentiated Tuscher and Farrer Formations, which can be divided into a lower and upper sequence. West of the Wilkin Ridge well, the nonmarine part of the Blackhawk Formation thickens and contains numerous thick coal beds and abundant carbonaceous, fine-grained clastic deposits. East of the Wilkin Ridge well, this coal-bearing interval thins markedly, and, east of the Green River, the sequence is very thin to absent.

Late Cretaceous movement of the Laramide San Rafael swell determined the thickness distribution of the nonmarine Cretaceous section in the southeastern part of the Uinta basin. Erosion of Upper Cretaceous rocks was most extensive along the Book Cliffs in the vicinity of Horse Canyon (sec. 9, T. 16 S., R. 14 E.), where only

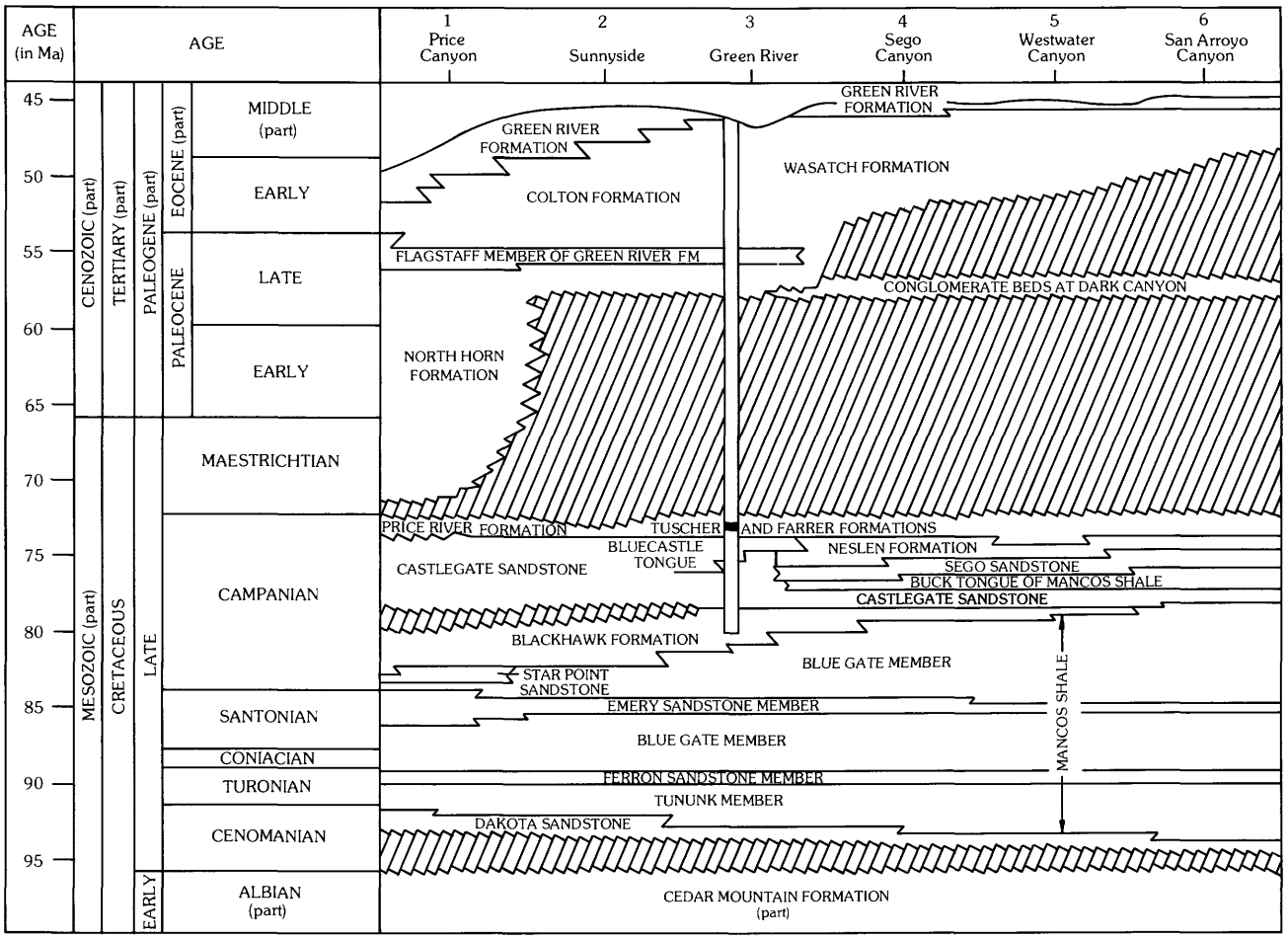


**Figure 2.** Schematic cross section showing time-stratigraphic relations of Cretaceous and Tertiary rocks along southern margin of Uinta basin. Outcrop localities are shown in figure 1; Wilkin Ridge well is near Green River location and is projected from subsurface to outcrop as shown by column. Shaded interval, cored sequence in well. Hachured area, unconformity. Modified from Fouch and others (1983).

330 ft (101 m) of Cretaceous rocks are preserved above the Bluecastle Tongue (Lawton, 1983). Along the Book Cliffs northwest of Horse Canyon, it is difficult to trace this interval and determine its thickness because of poor exposure and dense vegetation. At Range Creek, about 20 miles east of Horse Canyon, 1,020 ft (311 m) of Upper Cretaceous rocks are preserved above the Bluecastle Tongue (Lawton, 1983), and, at Wilkin Ridge, about 37 miles northeast of Horse Canyon, about 2,000 ft (610 m) of Upper Cretaceous rocks are preserved.

Late Cretaceous movement of the San Rafael swell (uplift) south of the Wilkin Ridge site caused appreciable local erosion of the upper, nonmarine part of the Cretaceous sequence. Thinning of the Upper Cretaceous section is most pronounced where the projected structural axis of the San Rafael uplift intersects outcrops of Upper Cretaceous rocks. The thin Upper Cretaceous section at Horse Canyon may result entirely from erosion or may be related, at least in part, to nondeposition. Along the outcrop, the nonmarine Cretaceous section thickens progressively eastward, and, near the Colorado–Utah State line, about 2,600 (792 m) of Cretaceous rocks overlie the Castlegate Sandstone. In the eastern part of the Uinta basin at the Natural Buttes gas field, about 35 miles east of the Wilkin Ridge well and 45 miles northwest of the State-line outcrops, 2,050 ft (625 m) of Cretaceous rocks overlie the Castlegate. Just east of the Douglas Creek arch in the Piceance basin, the nonmarine Cretaceous section is about 1,500 ft (457 m) thicker than in the central part of the Uinta basin (R.C. Johnson, oral commun., 1986).

## Geologic Nomenclature

Both a lack of subsurface information and the significant facies changes in the area around the Wilkin

Ridge well have caused confusion in picking unit boundaries and applying unit names. In this section, we outline the regional and local stratigraphy and nomenclature that are important in determining the selection of boundaries and nomenclature for Upper Cretaceous rocks of the Wilkin Ridge well.

Fouch and others (1983) and Lawton (1983) noted a threefold division of the Castlegate Sandstone in Price Canyon, northwest of Price, Utah: a basal unit of thickly bedded, laterally continuous sandstone that contains little interbedded fine-grained material; a middle unit of less laterally continuous sandstone interbedded with more abundant fine-grained material; and an upper unit of coarse-grained, thickly bedded, laterally continuous sandstone. The basal unit is equivalent to what is recognized as the Castlegate Sandstone along the eastern Book Cliffs, and the upper unit is equivalent to the Bluecastle Sandstone Tongue of the Castlegate Sandstone (Fouch and others, 1983), which can be traced eastward to Tuscher Canyon (fig. 2). The middle unit becomes less sandy and more organic rich eastward and is the landward equivalent of the Buck Tongue of the Mancos Shale and the Sego Sandstone west of their depositional pinchouts. Osterwald and others (1974) referred to this middle unit as the muddy member of the Price River Formation in the vicinity of Sunnyside and Horse Canyon; at Horse Canyon, Lawton (1983) referred to this same sequence as the Neslen Formation because it is depositionally similar and laterally equivalent to part of the Neslen Formation. Fisher and others (1960) did not extend the Neslen and Sego nomenclature west of the Green River, and, in the Wilkin Ridge area, this sequence is considered the middle unit of the Castlegate Sandstone. In the Wilkin Ridge well, the basal part of the Castlegate Sandstone is 265 ft (81 m) thick, the middle part 200 ft (61 m) thick, and the upper part, or Bluecastle Tongue, 135 ft (41 m) thick.

The undifferentiated Tuscher and Farrer Formations at Wilkin Ridge are equivalent to part of the Price River Formation to the west; the location of nomenclature change between these formations is arbitrary (fig. 2). These rocks represent the final phase of alluvial infilling of the Western Interior Cretaceous basin, and abundant, thick coal beds and carbonaceous-clastic deposits are rare. The boundary between the Tuscher and Farrer Formations originally was chosen principally on differences in topographic expression and the relative abundance and geometry of sandstone beds (Fisher and others, 1960). Outcrop studies show, however, that, because of regional lithofacies changes and variable weathering characteristics, these criteria cannot be used to select a consistent contact between the two units on the outcrop and they cannot be applied in the subsurface. In this study, therefore, the Tuscher and Farrer Formations are undifferentiated. Gamma-ray and resistivity well logs from the Wilkin Ridge well indicate a twofold division of the Tuscher-Farrer sequence: a lower, 452-foot-thick (138 m) interval composed of thin sandstone beds and abundant fine-grained deposits and an upper, 1,535-foot-thick (468 m) interval composed mostly of thick sandstone beds. Log signatures for the lower interval resemble those for the upper part of the Neslen Formation east of the Green River.

## Description of Core

The deepest core from the Wilkin Ridge well (11,185–11,230 ft, 3,409–3,431 m) penetrated the lower interval and consists of very fine to fine-grained sandstone, interbedded siltstone or sandstone and claystone, carbonaceous claystone, and thin (<0.5 ft, <0.15 m) coal beds. The sandstone units are 4–8 ft (1–2 m) thick, have sharp, slightly scoured bases, show no discernable upward change in grain size, and locally contain scattered clay rip-up clasts and coal clasts. Horizontal stratification is the dominant sedimentary structure, and low-angle cross-stratification is less common. Locally, these structures have been obscured or obliterated by soft-sediment deformation. Disseminated carbonaceous material and root casts occur throughout the sandstone units. The organic-rich interbedded siltstone or sandstone and claystone sequences are from less than 2 to as much as 8 ft thick (<1–2 m) and contain abundant root casts and possible burrows. Ripple stratification and wavy horizontal laminations are locally preserved, but most bedding has been obliterated by soft-sediment deformation. The carbonaceous claystone units are as thick as 5 ft (2 m) and are horizontally laminated where not penetrated by root casts. Thin coal beds (<0.5 ft (<0.15 m) thick) occur locally in the claystone units.

The core from the lower part of the upper unit (10,740–10,803 ft, 3,274–3,293 m) is composed almost entirely of fine- to medium-grained sandstone. Minor amounts of siltstone or claystone occur as rip-up clasts or as laminations in the sandstone. Individual sandstone units are 8–25 ft thick (2–8 m) and are defined by sharp, scoured basal contacts above which are abundant claystone rip-up clasts. Medium- to thin-bedded, medium- to low-angle cross-stratification and horizontal stratification are the dominant sedimentary structures in all sandstone units. Ripple stratification is common in the upper parts of units containing laminations of siltstone or claystone. Soft-sediment deformation is present locally but is not as abundant as in the deepest cored sequence.

A thin interval (10,273–10,295 ft, 3,131–3,138 m) containing a single sequence of sandstone that grades upward into carbonaceous claystone was cored in the upper part of the upper unit of the Tuscher and Farrer Formations. The sandstone is 8 ft (2 m) thick, has a sharp

basal contact, and fines upward from medium to fine grained at its base to very fine grained at its top. Medium- to thin-bedded, medium- to low-angle cross-stratification in the lower few feet of the sandstone is replaced upward by horizontal and ripple stratification. Root casts are also common in the upper part of the sandstone. Interbedded sandstone and claystone overlie the sandstone, and abundant root casts, ripple stratification, and laminations of coaly material characterize these interbeds. The amount of sandstone gradually decreases upward, and the claystone at the top of the sequence is very carbonaceous, contains coal fragments, and has horizontal laminations locally disrupted by root casts and deformation.

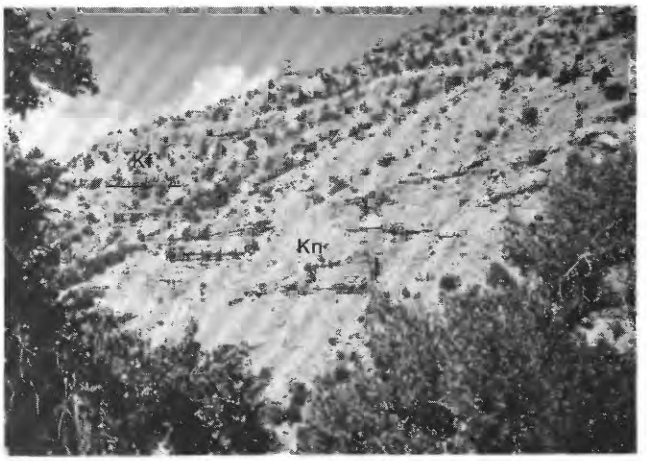


**Figure 3.** Outcrop of Neslen Formation exposed on north side of Cottonwood Canyon, Grand County, Utah; view is looking north. These rocks are similar to cored sequences in lower part of the undifferentiated Tuscher and Farrer Formations in Wilkin Ridge well. The transition between the Neslen (Kn) and Farrer (Kf) Formations is gradational. The more resistant units in the dominantly slope forming Neslen Formation show lateral-accretion crossbedding and were deposited by meandering channels. The dark zones at the base or top of channel deposits are thin coal beds.

## SEDIMENTOLOGY

Environments during Tuscher-Farrer deposition can be inferred from the cores, geophysical logs, and outcrop equivalents. The lower part of the Tuscher-Farrer sequence (from the base of the formation to a depth of 11,090 ft, 3,380 m) was deposited on extensive floodplains crossed by shallow, meandering rivers. The abundance of organic-rich, extensively rooted beds in the lowest unit indicates deposition on floodplains containing levees, both well- and poorly drained swamps, crevasse splays, and freshwater lakes. Sandstone units having sharp scour bases are of channel origin, but both their thinness and the abundance of low-flow-regime sedimentary structures suggest deposition in shallow crevasse channels that formed adjacent to larger channels. Outcrop sequences from the Neslen Formation are similar to those observed in core of the lower units (fig. 3). Relatively thin, locally stacked channel-sandstone units that exhibit well-developed large-scale lateral-accretion cross-stratification are surrounded by carbonaceous, fine-grained, slope-forming units. A lower-alluvial-plain environment, characterized by relatively shallow meandering streams flowing through extensive vegetated floodplains, has been inferred for the upper part of part of the Neslen Formation in the Tuscher and Sego Canyon areas (K.J. Franczyk, unpub. data, 1985) and probably existed in the Wilkin Ridge area during deposition of the lower part of the undifferentiated Tuscher and Farrer Formations. Mineralogic compositions of sandstones in the lowest cored unit are similar to those of sandstones in the Neslen Formation and are discussed later.

Both geophysical logs and petrographic studies of core from the upper part of the Tuscher and Farrer Formations indicate that stacked sandstone sequences, some as thick as 80 ft (24 m), predominate; shaly material is significantly less common than in the lower unit but is locally present. The transition from the lower to the upper part of the Tuscher and Farrer Formations is gradational and is represented in outcrop by the transition from the Neslen to Farrer Formations (fig. 4). This transition indicates an increase in the clastic supply transported by deeper meandering rivers (Pitman, Anders, and others, 1986) whose extensive migrations across the alluvial plain prevented accumulations of thick overbank deposits. Although sandstone predominates in the upper unit, geophysical logs indicate that intervals as thick as 160 ft (49 m) are composed dominantly of fine-grained shaly material and only minor sandstone. These fine-grained overbank deposits (fig. 5) formed when major rivers avulsed and abandoned an area or when changes in rates of sediment supply or subsidence caused a decrease in channel migration. Organic-rich floodplain deposits, potential hydrocarbon source rocks, occur locally in the upper unit of the Tuscher and Farrer Formations at Wilkin Ridge, but, because they vary greatly in thickness and lateral extent, it is difficult to predict their location on a regional scale.

The increase in abundance of sandstone from the lower to upper part of the undifferentiated Tuscher and Farrer Formations in the Wilkin Ridge core is accompanied by a change in sandstone mineralogy similar to that observed in outcrop between the Bluecastle Tongue of the Castlegate Sandstone and the Farrer Formation or between the Neslen and the Farrer Formations east of the Bluecastle pinchout. Lawton (1983) and Dickinson and others (1986) interpreted the western and northwestern thrust belt to be the Bluecastle and Neslen source area. In their interpretation, this source area shifted at the beginning of Farrer deposition to the southern thrust belt

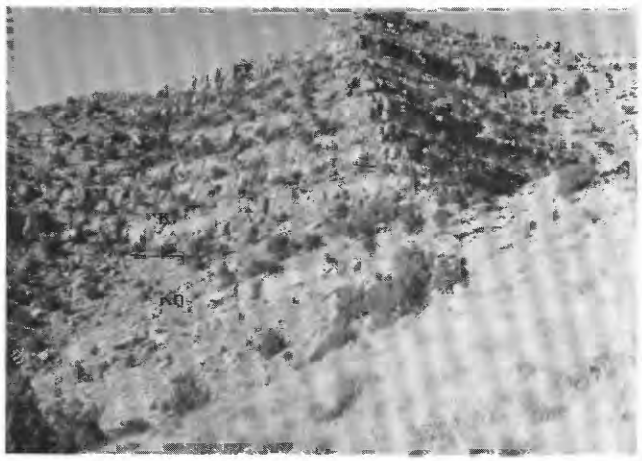

**Figure 4.** Gradational contact between Neslen (Kn) and Farrer (Kf) Formations, as exposed on north side of Cottonwood Canyon, Grand County, Utah; view is looking north. The lower part of Tuscher Formation (Kt) is just visible on skyline. Fluvial sandstones in Farrer and Tuscher Formations are laterally extensive and locally stacked.

and areas outside of the thrust belt. Our study suggests that, in the Wilkin Ridge area, the western and northwestern thrust belt continued to supply sediment during early stages of Farrer deposition.

## FRAMEWORK MINERALOGY

Sandstones representative of the lower and upper units of the undifferentiated Tuscher and Farrer Formations in the Wilkin Ridge well were studied petrographically to determine detrital and authigenic mineral compositions (table 1) and their effects on reservoir quality. In the lower unit, fine-grained, moderately well sorted sandstones are composed mostly of quartz grains, varying proportions of sedimentary lithic fragments, and matrix; they are devoid of feldspar. This distinctive mineral suite has previously been reported only for the Neslen Formation (Keighin and Fouch, 1981; Lawton, 1983; Pitman and others, 1987). In the upper unit, fine- to medium-grained, moderately to well-sorted sandstones are composed of monocrystalline quartz, feldspar, and lithic fragments, mostly of sedimentary and volcanic origin, a mineral assemblage characteristic of the Tuscher and Farrer Formations in other parts of the basin (Keighin and Fouch, 1981; Lawton, 1983; Pitman, Anders, and others, 1986). Most of the mineral constituents except feldspar in the Tuscher and Farrer were derived from sedimentary and igneous source terranes in the Sevier orogenic belt in western Utah; some feldspar and volcanic lithic fragments most likely originated in rocks previously exposed in provinces southwest of the thrust belt (Fouch and others, 1983; Dickinson and others, 1986; Pitman, Anders, and others, 1986).

**Figure 5.** Typical sequence of overbank deposits preserved between extensive fluvial sandstones in the Tuscher and Farrer Formations in outcrops on north side of Cottonwood Canyon, Grand County, Utah. Siltstones and mudstones generally are greenish gray and contain little organic material; coal beds are rare, but fragments of coaly material are locally present. Thick sandstone in photograph is part of a crevasse channel deposit. Backpack (lower part of photograph) gives scale.

A ternary diagram showing the relative proportions of quartz, feldspar, and lithic fragments delineates mineralogic variations within and between the lower and upper sandstone units (fig. 6). According to the classification scheme of Folk (1974), sandstones in the lower unit are quartzarenites and sublitharenites; these lithologies, which show only minor diagenetic alterations, are typical of the Neslen Formation and have not been previously reported for the Tuscher and Farrer Formations. Sandstones in the upper unit are characterized by two mineral populations. In the upper part of the upper unit, sandstones contain significantly altered and dissolved feldspar grains and lithic fragments, indicating the rocks have undergone intense diagenetic modification; these sandstones are now sublitharenites. In contrast, the lower part of the upper unit contains sandstones that have undergone only moderate diagenetic alteration; these rocks are

**Table 1.** Mineralogic compositions of sandstones in the undifferentiated Tuscher and Farrer Formations, Wilkin Ridge well

[Petrographic properties in percent; Tr, trace amount. Thin sections were impregnated with blue epoxy and then stained with potassium ferrocyanide and alizarin red to identify carbonate minerals and with potassium cobaltinitrate to distinguish between potassium and sodium feldspars. Three hundred points were counted per thin section]

| Depth (meters) | Depth (feet) | Quartz | Potassium feldspar | Plagioclase | Matrix | Rock fragments | Chert | Dolomite | Calcite | Visible pore space | Anhydrite | Other |
|---|---|---|---|---|---|---|---|---|---|---|---|---|
| | | | | | **Upper unit** | | | | | | | |
| 3,134.0 | 10,282.0 | 50 | 0 | 0 | 46 | 2 | 0 | 0 | 0 | 0 | 0 | 3 |
| 3,134.3 | 10,283.0 | 58 | 0 | 0 | 37 | 0 | 2 | 0 | 0 | 0 | 0 | 3 |
| 3,134.7 | 10,284.5 | 78 | 0 | Tr | 0 | 8 | 3 | 1 | 1 | 8 | 0 | 1 |
| 3,134.9 | 10,285.0 | 73 | 0 | Tr | 0 | 6 | 5 | 0 | 0 | 14 | 0 | 1 |
| 3,135.4 | 10,286.7 | 72 | 0 | 1 | 0 | 7 | 7 | 0 | 2 | 9 | 0 | 1 |
| 3,136.0 | 10,288.6 | 69 | 0 | 1 | 7 | 6 | 2 | 10 | 2 | 1 | 0 | 2 |
| 3,136.4 | 10,290.0 | 69 | 0 | 2 | 0 | 7 | 8 | 4 | 3 | 6 | 2 | 0 |
| 3,137.3 | 10,293.0 | 80 | 0 | 1 | 1 | 4 | 5 | 3 | 0 | 4 | 2 | 0 |
| 3,137.6 | 10,294.0 | 79 | 0 | 2 | 0 | 3 | 3 | 2 | 0 | 8 | 1 | 2 |
| 3,138.1 | 10,295.5 | 69 | 0 | 2 | 0 | 11 | 5 | 1 | 0 | 10 | 0 | 1 |
| 3,138.7 | 10,297.5 | 75 | 0 | 2 | 0 | 5 | 8 | 0 | 0 | 5 | 4 | 1 |
| 3,139.0 | 10,298.7 | 78 | 0 | 2 | 0 | 3 | 7 | 1 | Tr | 7 | 2 | 0 |
| 3,139.4 | 10,299.8 | 74 | 0 | 1 | 0 | 10 | 4 | 3 | 0 | 7 | Tr | 1 |
| 3,140.1 | 10,302.0 | 52 | 0 | 5 | 0 | 22 | 4 | 1 | Tr | 13 | 0 | 1 |
| 3,140.8 | 10,304.5 | 41 | 0 | 3 | 20 | 20 | 9 | 5 | 0 | 0 | 0 | 2 |
| 3,273.6 | 10,740.3 | 53 | 0 | 9 | 1 | 14 | 4 | 6 | 2 | 6 | 0 | 4 |
| 3,274.2 | 10,742.0 | 42 | 1 | 4 | 17 | 13 | 3 | 12 | 0 | 0 | 0 | 8 |
| 3,275.1 | 10,745.1 | 50 | 0 | 8 | 0 | 16 | 5 | 4 | 2 | 13 | 0 | 2 |
| 3,275.8 | 10,747.4 | 49 | 0 | 8 | 0 | 14 | 4 | 8 | 3 | 11 | 0 | 2 |
| 3,276.5 | 10,749.5 | 46 | 0 | 8 | 0 | 11 | 3 | 12 | 6 | 11 | 0 | 3 |
| 3,277.0 | 10,751.2 | 44 | 0 | 7 | 3 | 13 | 5 | 9 | 14 | 1 | 0 | 4 |
| 3,278.2 | 10,755.3 | 33 | 3 | 20 | 10 | 14 | 7 | 3 | 0 | 4 | 0 | 8 |
| 3,278.8 | 10,757.3 | 50 | 0 | 16 | 2 | 11 | 9 | 2 | 1 | 8 | 0 | 2 |
| 3,279.6 | 10,759.7 | 37 | 0 | 14 | 3 | 16 | 7 | 3 | 1 | 15 | 0 | 4 |
| 3,280.7 | 10,763.5 | 46 | 0 | 12 | 2 | 11 | 9 | 4 | 2 | 10 | 0 | 4 |
| 3,281.3 | 10,765.4 | 45 | 0 | 15 | 3 | 11 | 9 | 6 | 3 | 6 | 0 | 3 |
| 3,281.9 | 10,767.3 | 29 | 1 | 11 | 18 | 9 | 4 | 6 | 1 | 2 | 0 | 18 |
| 3,282.8 | 10,770.2 | 44 | 3 | 8 | 2 | 17 | 6 | 7 | 0 | 8 | 0 | 7 |
| 3,283.5 | 10,772.7 | 52 | 0 | 7 | 2 | 16 | 6 | 6 | 3 | 5 | 0 | 3 |
| 3,284.0 | 10,774.2 | 47 | 0 | 9 | 3 | 17 | 7 | 6 | 3 | 5 | 0 | 4 |
| 3,284.8 | 10,776.8 | 52 | 0 | 9 | 1 | 14 | 5 | 4 | 2 | 8 | 0 | 4 |
| 3,285.2 | 10,778.3 | 48 | 0 | 7 | 3 | 16 | 7 | 5 | 2 | 5 | 0 | 6 |
| 3,286.2 | 10,781.4 | 40 | 0 | 8 | 7 | 17 | 4 | 6 | 1 | 7 | 0 | 9 |
| 3,286.9 | 10,783.7 | 46 | 0 | 8 | 2 | 19 | 4 | 5 | 1 | 10 | 0 | 4 |
| 3,287.3 | 10,785.2 | 50 | 0 | 5 | 2 | 14 | 3 | 11 | 1 | 10 | 0 | 4 |
| 3,288.4 | 10,788.7 | 49 | 0 | 10 | 2 | 15 | 9 | 3 | 0 | 10 | 0 | 3 |
| 3,288.9 | 10,790.2 | 48 | 0 | 15 | 1 | 13 | 5 | 4 | 1 | 10 | 0 | 2 |
| 3,289.2 | 10,791.3 | 50 | 0 | 10 | 2 | 12 | 10 | 2 | 2 | 8 | 0 | 4 |
| 3,289.9 | 10,793.5 | 46 | 0 | 9 | 2 | 4 | 11 | 2 | 3 | 10 | 0 | 3 |
| 3,290.3 | 10,795.0 | 51 | 0 | 10 | 1 | 16 | 6 | 2 | 3 | 8 | 0 | 4 |
| 3,290.7 | 10,796.3 | 47 | 2 | 9 | 1 | 14 | 9 | 6 | 2 | 4 | 0 | 7 |
| 3,291.2 | 10,797.8 | 45 | 0 | 9 | 5 | 14 | 7 | 6 | 3 | 6 | 0 | 4 |
| 3,292.9 | 10,800.6 | 41 | 0 | 9 | 7 | 13 | 7 | 6 | 5 | 6 | 0 | 6 |
| | | | | | **Lower unit** | | | | | | | |
| 3,411.3 | 11,192.0 | 45 | 0 | 0 | 52 | Tr | 3 | 0 | 0 | 0 | 0 | 0 |
| 3,411.9 | 11,194.0 | 56 | 0 | 0 | 40 | 1 | 2 | 1 | 0 | 0 | 0 | 1 |
| 3,412.9 | 11,197.3 | 69 | 0 | 0 | 15 | 2 | 1 | 5 | Tr | Tr | 0 | 7 |
| 3,415.1 | 11,204.5 | 77 | 0 | 0 | 13 | 3 | 1 | 3 | 0 | 0 | 0 | 3 |
| 3,417.0 | 11,211.0 | 70 | 0 | 0 | 17 | 3 | 2 | 8 | 0 | 0 | 0 | 1 |
| 3,418.6 | 11,215.7 | 65 | 0 | 0 | 12 | 2 | 2 | 13 | 3 | Tr | 0 | 4 |
| 3,421.1 | 11,224.3 | 89 | 0 | 0 | 7 | Tr | 1 | 1 | Tr | Tr | 0 | 1 |

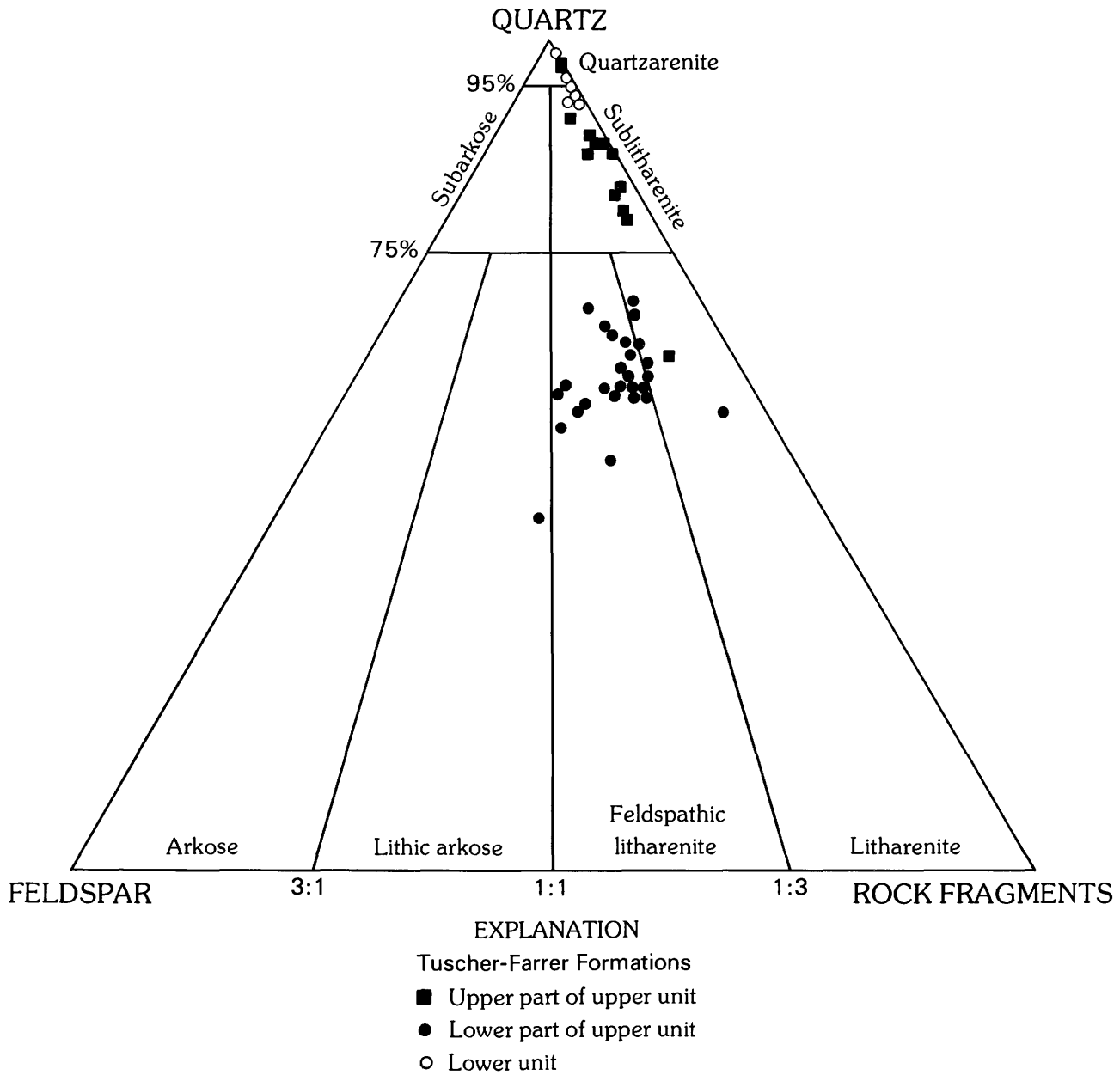


**Figure 6.** Classification of sandstones in the undifferentiated Tuscher and Farrer Formations in the Wilkin Ridge well. Modified from Folk (1974).

predominantly feldspathic litharenites. Both lithologies in the upper unit are similar to those of the Tuscher and Farrer Formations in outcrop along the Book Cliffs in the southern part of the Uinta basin and in the subsurface east of the Green River.

## Quartz

Detrital quartz is a dominant framework grain and comprises an average of 67 percent of the whole rock in the lower cored unit in the Wilkin Ridge well. In the upper unit, quartz is less abundant and constitutes 29 to 80 percent. Quartz grains in both units typically are subangular to moderately rounded and range from very fine to medium in size. Most are monocrystalline, have slight undulatory extinction, and contain minute vacuoles.

## Feldspar

Feldspar is absent in sandstones in the lower unit of the Tuscher and Farrer Formations, but plagioclase constitutes from trace amounts to 21 percent and

potassium feldspar a few percent in the upper unit. Most plagioclase grains are individual, untwinned, subangular to subrounded, and fresh to extensively altered. Altered plagioclase grains show evidence of replacement by sericite, carbonate, barite or anhydrite, and the effects of partial to complete dissolution. Potassium feldspar grains are both twinned and untwinned and similar in size and shape to plagioclase. Most grains are orthoclase, although a few grains of microcline were recognized by their grid twinning. Because both sodium and potassium feldspars are susceptible to leaching, potassium feldspar typically has undergone more extensive dissolution such that only a skeleton of the original grain is preserved. Rare grains of feldspar within volcanic rock fragments also appear to have undergone some dissolution.

### Lithic Fragments

Lithic fragments of diverse origin are abundant in the undifferentiated Tuscher and Farrer Formations, constituting from a trace to 3 percent of the grains in the lower unit and from 2 to 22 percent of the grains in the upper unit. The most abundant grains are of sedimentary origin and include polycrystalline carbonate, argillaceous shale, and mudstone and siltstone. Many have been extensively altered to sericite and are mechanically unstable; as a result, they have been deformed between framework grains to form a pseudomatrix or have been partly to completely dissolved. Chert forms a significant proportion (2–11 percent) of the lithic fragments in the upper unit. Much of the chert is unaltered and composed of interlocking microcrystalline quartz crystals that range from cryptocrystalline (<0.05 mm) to polycrystalline (<0.1 mm). It is commonly difficult to differentiate between polycrystalline quartz and coarse-crystalline chert because of the gradation in grain size. Some chert grains are medium to very dark brown as a result of inclusions of carbonaceous material, and some grains are cut by veins of quartz. A few chert grains are micaceous or contain small dolomite rhombs that grew after sediment deposition. In some sandstones, chert grains contain fossil crinoid fragments that have been locally dissolved. These fossiliferous grains perhaps are fragments of silicified limestone reworked from Paleozoic carbonate rocks. In the upper unit, other lithic fragments include plutonic igneous fragments containing feldspar and quartz, polycrystalline quartz grains having straight to undulose extinction and curved to sutured boundaries between individual crystals, and numerous altered volcanic grains composed of feldspar and chlorite.

### Matrix

Varying amounts of detrital matrix are present in Tuscher and Farrer sandstones, and, although detrital matrix locally constitutes as much as 52 percent by volume, overall it is a minor constituent. Pseudomatrix resulting from mechanical deformation of unstable lithic fragments is common, particularly in the lower unit, because of the presence of argillaceous grains. In sandstones containing abundant pseudomatrix and detrital matrix, porosity and permeability have been significantly reduced.

### Cements

Secondary quartz, developed as syntaxial overgrowths on detrital grains, locally is a widespread mineral cement in sandstones in the lower and upper units of the Tuscher and Farrer Formations. It is most abundant in rocks containing only small amounts of matrix and compressible framework grains. In areas where quartz overgrowths are well developed, they typically are difficult to distinguish from the detrital grains, and, as a result, their relative abundance is uncertain. Partly abraded grain overgrowths in optical continuity with framework quartz grains in the upper unit suggest some grains and overgrowths may have been recycled from older terrane. Most quartz overgrowths are recognized by their euhedral, rhombohedral, and prismatic crystal faces. In sandstones in which discrete grain overgrowths have coalesced to form a cement, the effects of pressure solution may be seen. In the upper unit, quartz overgrowths have clearly developed in sandstones in which the exposed grain surfaces were not coated with early authigenic chlorite or the amounts of detrital matrix and mechanically unstable lithic grains were minimal. In the lower part of the upper unit, overgrowths commonly contain dissolution voids created by the removal of replacement anhydrite and possibly barite or have been etched as a result of the dissolution of precursor carbonate cement.

A mineralogically complex assemblage of iron-rich and iron-poor carbonate cements was observed in sandstones in the upper unit of the undifferentiated Tuscher and Farrer Formations; most sandstones in the lower unit contain only minor amounts of carbonate. In the upper unit, authigenic ferroan calcite is locally abundant and constitutes from trace amounts to 14 percent; dolomite is less abundant and constitutes from 1 to 12 percent. Because it is difficult to differentiate between grains of detrital dolomite and authigenic anhedral replacement dolomite, their relative abundances are only approximate.

In sandstones in the upper unit, two generations of calcite can be distinguished based on mode of occurrence and texture. Rare iron-free calcite occurs as relicts surrounded by optically continuous ferroan calcite (fig. 7). Most calcite now in the sandstones is enriched in iron and forms a poikilotopic spar cement that embays grain margins and cleavage traces or replaces framework grains

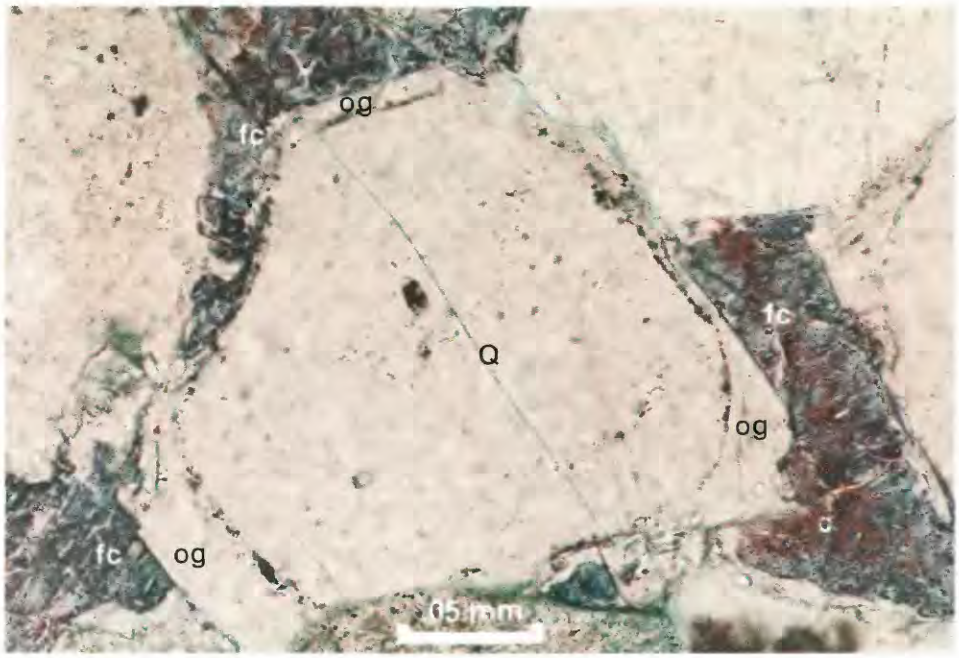


**Figure 7.** Replacement of relict iron-free calcite pore-filling cement (c; red stain) by iron-bearing calcite (fc; blue stain). Note that secondary quartz overgrowths (og) predate development of authigenic calcite. Q, quartz.

such as feldspar. The relative distribution of ferroan calcite varies: wherever it is abundant, framework-grain alteration and compaction usually have been minimal. In many sandstones, ferroan calcite is preserved only locally in pores lined with authigenic iron chlorite, as relicts in secondary voids, and as a grain replacement. In sandstones having well-developed inter- and intragranular porosity, dissolution features that closely resemble the texture of undissolved carbonate and calcite remnants that occupy pores both are evidence that calcite was a preexisting cement.

In the upper part of the upper unit, the sulfate minerals anhydrite and barite are present locally from trace amounts to 4 percent. The presence of these minerals positively correlates with the occurrence of small amounts of bitumen, although neither anhydrite nor barite was observed in direct contact with kerogen. The mode of occurrence of anhydrite and barite ranges from small scattered patches to large poikilotopic crystals that replace and surround framework grains and early silica and carbonate cement (figs. 8–10). In some sandstones, either one or both of these minerals have been partly to completely dissolved. Irregular clay-filled voids that cut across detrital quartz grains and overgrowths are features closely resembling the texture of anhydrite where it is still preserved.

### Clays

The principal clay-mineral assemblage in the undifferentiated Tuscher and Farrer Formations is composed of illite, chlorite, and mixed-layer illite-smectite. Thin, isopachous rims of authigenic chlorite and pore-fill cement are preserved locally in some sandstones in the upper unit. X-ray diffraction analysis indicates that all chlorite is well crystallized and iron rich.

Individual chlorite rims typically are composed of pseudohexagonal platelets that are oriented perpendicular to grain surfaces forming a cement. Quartz overgrowths are rare in sandstones displaying widespread rim cement. In areas where chlorite is abundant, it lines pores and coats framework grains except where the grains are in contact with each other. Pores lined with chlorite often contain carbonate relicts or are filled by a late generation of chlorite. If voids are open, the rim cement may be crushed or contorted due to mechanical compaction.

Authigenic illite and illite-smectite are abundant clay-mineral constituents throughout the undifferentiated Tuscher and Farrer Formations. They commonly are attached to authigenic chlorite grain surfaces, display a fibrous habit in pores, or are distributed as thin coats on detrital grains. Illite and illite-smectite are particularly widespread in secondary pores that contain evidence for preexisting carbonate and sulfate cement.

## MECHANICAL COMPACTION

The effects of mechanical compaction are evident in all of the cored sandstones from the Wilkin Ridge well

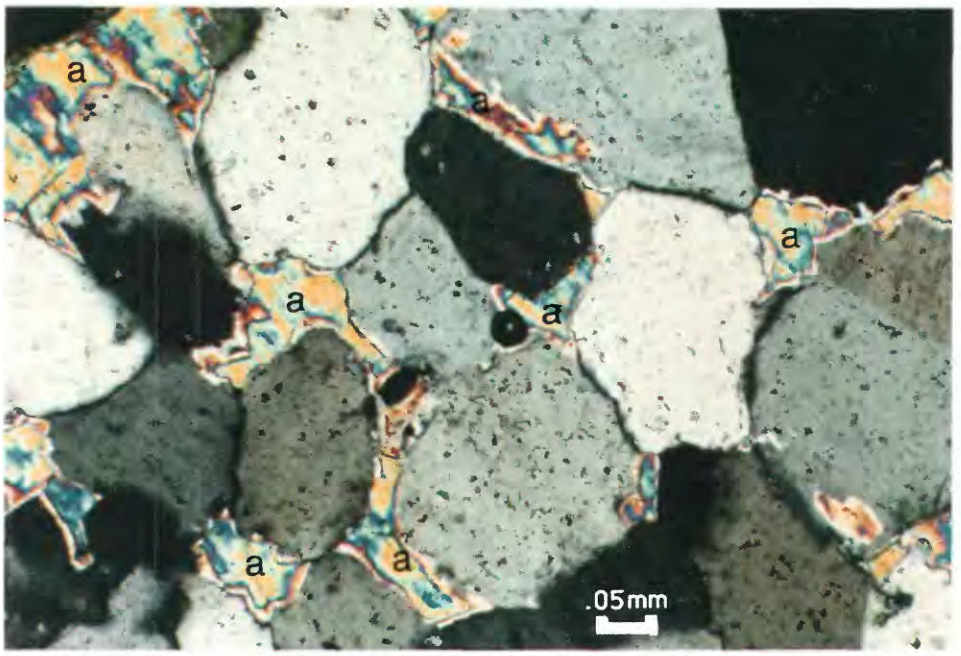


**Figure 8.** Late-stage poikilotopic anhydrite cement (a).

and generally are more pronounced as burial depth increases. A few sandstones containing framework grains floating in carbonate cement and an early generation of iron chlorite display only slight to moderate compaction effects, principally grain rotation.

## DIAGENESIS

Based on our petrographic studies, the diagenetic history of Upper Cretaceous sandstones in the undifferentiated Tuscher and Farrer Formations in the central Uinta basin appears to be more complex than that of rocks of similar age and origin that have been less deeply buried in the eastern part of the Uinta basin (Keighin and Fouch, 1981; Pitman, Goldhaber, and Fouch, 1986; Pitman and others, 1987). Sandstone paragenesis in the lower unit includes: (1) mechanical compaction of framework grains, (2) quartz overgrowths developed locally on framework quartz grains, (3) authigenic carbonate preserved as a pore fill and as a replacement mineral, and (4) authigenic illite and chlorite occluding secondary pores. These diagenetic features also are characteristic of the underlying Neslen Formation.

Sandstones in the upper unit, particularly those that contain bitumen, have undergone a more complex diagenetic history that includes: (1) mechanical compaction of detrital grains, (2) development of secondary quartz overgrowths, (3) formation of iron chlorite rim cement, (4) precipitation and subsequent dissolution of nonferroan and ferroan carbonate, (5) formation of authigenic illite and chlorite in secondary pores, (6) crystallization and dissolution of anhydrite and barite, and (7) maturation and generation of hydrocarbons. The chemically diverse mineral assemblage that characterizes the upper unit suggests diagenesis occurred under the influence of depositional fluids whose compositions evolved during burial. Most of the constituents necessary for crystallization of the authigenic minerals probably either were derived from the redistribution of ions within the sandstones or were transported locally from interbedded shales.

### Silica Cementation

Secondary quartz was the earliest cement to form in most sandstones. In the upper unit, textural relations between discrete quartz overgrowths and other mineral cements indicate secondary quartz predated formation of all mineral cements except iron chlorite. Pressure solution was evidently important in the development of secondary quartz in both units. Well-developed concavo-convex grain contacts and sparse sutured contacts suggest silica may have precipitated from migrating pore water, as well as from oversaturated fluids resulting from local pressure solution. At shallow burial depths, the transformation of smectite to illite may have provided an additional source of silica. Later in the burial history, silica also may have been derived from dissolution of feldspar.

### Carbonate and Sulfate Mineral Development

At least two episodes of calcite crystallization occurred in the Tuscher and Farrer Formations at different

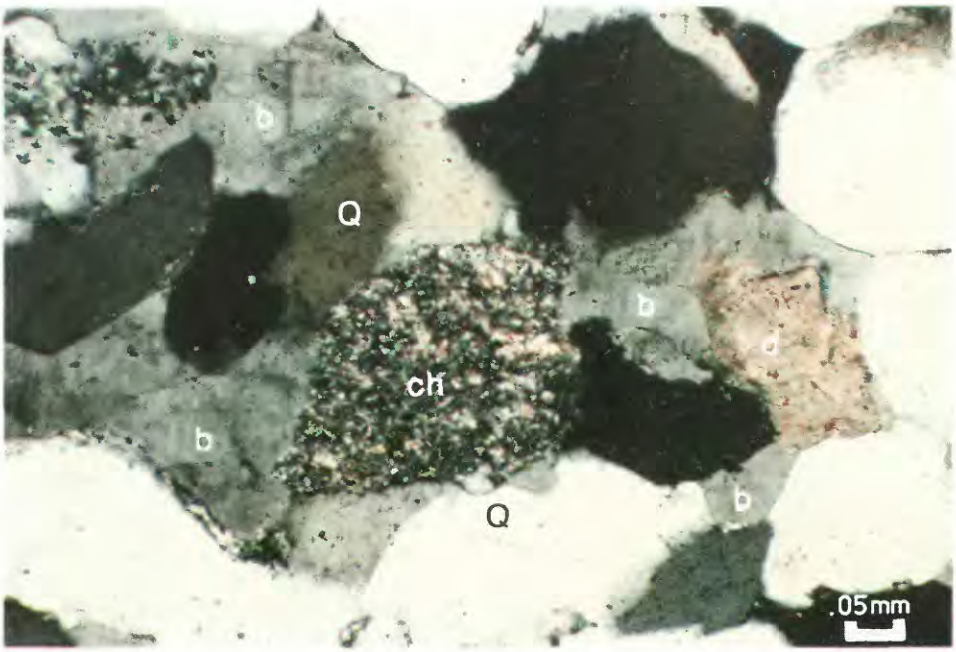


**Figure 9.** Barite (b) replacing authigenic dolomite (d) and detrital framework grains of quartz (Q) and chert (ch).

times and at different depths during burial. Nonferroan calcite, the earlier carbonate, most likely precipitated from near-surface waters during early diagenesis at shallow burial depths before clay-mineral transformations and release of iron. At greater burial depths during a later stage of diagenesis, ferroan calcite, now the most abundant carbonate cement, formed from iron-bearing fluids. Ferroan dolomite also formed late in the burial history, probably from the same diagenetic fluids that precipitated ferroan calcite. In sandstones exhibiting extensive cementation by ferroan calcite, the relatively minor chemical alteration and mechanical compaction of framework constituents suggest the ferroan calcite probably was deposited relatively early in the burial history, before significant compaction occurred. The ferroan calcite may have absorbed a considerable amount of overburden pressure during burial and thus prevented further mechanical compaction in the sandstones. The relative abundance of carbonate and the sparsity of point contacts between individual detrital grains indicate that porosities and permeabilities were high when the sandstones were initially cemented; these initial high porosities and permeabilities are further evidence that a large fraction of the carbonate, as calcite, formed during an early stage of diagenesis.

Cementation by ferroan calcite is incomplete in many sandstones; relict calcite in intergranular pores suggests that, in selected intervals, a period of dissolution occurred. Replacement calcite that formed along cleavage traces in individual feldspar grains also is commonly leached. Many partly to completely dissolved feldspar grains may have originally been more calcic than adjacent grains that show virtually no effects of leaching or surface etching. The dissolution of ferroan and nonferroan calcite was an important diagenetic event in the reservoir development of the upper unit because it resulted in a substantial increase in overall porosity and permeability of the sandstones. Dissolution of carbonate cement and framework grains probably occurred at moderate rather than shallow burial depths because most feldspar relicts are delicate structures showing little evidence of the mechanical compaction that would result from surface or near-surface leaching. Clay-mineral and organic reactions in shales during diagenesis may have produced sufficient water, organic acids, and complexing agents to dissolve chemically unstable framework grains and authigenic cements in nearby sandstones (Siebert, 1984).

#### Carbon and Oxygen Isotopes

Carbon and oxygen isotope compositions were determined for selected ferroan calcite and dolomite samples in order to establish the chemical conditions that governed carbonate cementation (table 2). The range in compositions is similar to those reported by Pitman, Goldhaber, and Fouch (1986) and Pitman and others

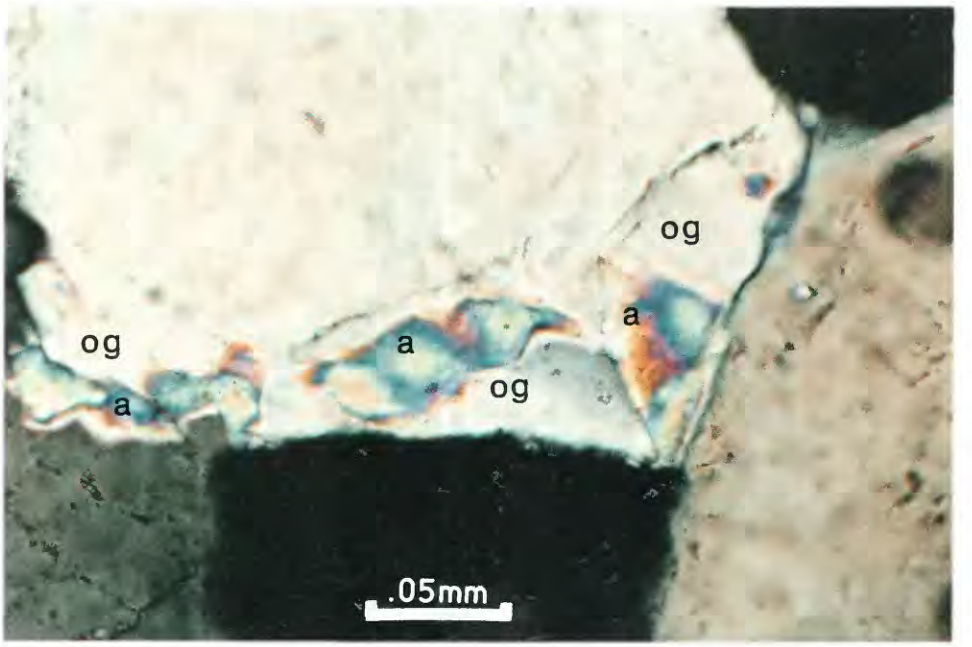


**Figure 10.** Replacement of secondary quartz overgrowths (og) by authigenic anhydrite (a).

(1987) for temporally equivalent rocks farther east in the basin. In the lower unit, $\delta^{13}C$ ranges from –0.99 to –3.25 per mil and $\delta^{18}O$ ranges from –9.83 to 13.36 per mil. Calcite in sandstones from the lower part of the upper unit displays isotope compositions similar to those for calcite from sandstones from the lower unit, from –1.06 to –2.12 per mil $\delta^{13}C$ and from –10.28 to –14.70 per mil $\delta^{18}O$. Sandstones from the upper part of the upper unit contain calcite that is distinctly lighter than the underlying rocks; $\delta^{13}C$ varies from –3.95 to –7.75 per mil, and $\delta^{18}O$ from –12.21 to –14.04 per mil.

Isotope compositions for dolomite closely approximate those for calcite. In the lower unit, $\delta^{13}C$ ranges from +0.24 to –3.53 per mil and $\delta^{18}O$ from –9.83 to –13.36 per mil. In the lower part of the upper unit, dolomite displays isotopically heavier compositions varying from –0.01 to –0.66 per mil $\delta^{13}C$ and from –5.41 to –7.36 per mil $\delta^{18}O$. Most dolomite in the upper part of the upper unit is isotopically light compared to the underlying rocks, and ranges from –1.16 to –5.32 per mil $\delta^{13}C$ and from –6.88 to –11.99 per mil $\delta^{18}O$.

A crossplot of $\delta^{13}C$ and $\delta^{18}O$ compositions for the Tuscher and Farrer Formations is shown in figure 11. Calcite compositions that lie along the upper linear trend represent early carbonate that has remained virtually unaltered since deposition, whereas compositions that either cluster along the dashed line or in the extreme left corner of the diagram represent calcite that has undergone diagenetic modification during burial.

Isotope compositions of dolomite also form a distinct linear trend (fig. 11). The isotopically heaviest compositions represent dolomite of detrital origin, whereas the lighter compositions (along the dashed part of the line) represent dolomite affected by diagenetic alteration. The linear trends along which most samples plot suggest that authigenic carbonate formed dominantly under the influence of meteoric waters.

#### Carbon Isotopes

The variation in $\delta^{13}C$ reflects the contribution of carbon from different sources. Isotopically heavy carbon (about –1.0 per mil) probably was derived from dissolved marine carbonate species, inasmuch as the $\delta^{13}C$ compositions are within the range commonly reported for normal marine carbonate sediments (Gross, 1964). Isotopically lighter carbon compositions in the upper part of the upper unit and locally in the lower unit characterize sandstones having somewhat high initial porosity and permeability. Hence, these sandstones probably were locally affected by a higher degree of water–rock interaction. It is also possible that the fluids contained a small amount of organic carbon.

The $\delta^{13}C$ compositions for dolomite in the lower unit and in the lower part of the upper unit are very similar to those associated with marine dolomite (Weber, 1964). Petrographic observations indicate that most of the dolomite is detrital and only a small fraction is authigenic. This isotopically heavy carbon most likely was

**Table 2.** Carbon and oxygen isotope analyses for selected samples of calcite and dolomite from sandstones in the undifferentiated Tuscher and Farrer Formations, Wilkin Ridge well
[Asterisk (*), sample having unusually light isotope composition; leaders (---), not determined. Parentheses enclose results of duplicate analyses]

| Depth (meters) | Depth (feet) | Calcite | | Dolomite | |
|---|---|---|---|---|---|
| | | $\delta^{13}C_{PDB}$ | $\delta^{18}O_{PDB}$ | $\delta^{13}C_{PDB}$ | $\delta^{18}O_{PDB}$ |
| | | **Upper unit** | | | |
| *3,136.0 | 10,288.6 | -3.95 | -12.39 | -1.16 | -7.12 |
| *3,136.4 | 10,290.0 | -6.66 | -14.04 | -3.22(-3.42) | -9.75(-9.96) |
| *3,137.3 | 10,293.0 | --- | --- | -3.22 | -10.43 |
| *3,137.6 | 10,294.0 | --- | --- | -2.71 | -9.39 |
| *3,138.7 | 10,297.5 | --- | --- | -5.32 | -10.17 |
| *3,030.8 | 10,298.7 | -7.75 | -12.21 | -3.28 | -10.55 |
| *3,139.4 | 10,299.8 | --- | --- | -4.33 | -11.99 |
| 3,140.8 | 10,304.5 | --- | --- | -1.32 | -6.88 |
| 3,273.6 | 10,740.3 | -1.22 | -10.54 | -0.31 | -6.28 |
| 3,277.0 | 10,751.2 | -2.06 | -14.00 | -0.66 | -7.36 |
| 3,279.6 | 10,759.7 | -1.61 | -12.80 | -0.27 | -6.78 |
| 3,282.7 | 10,770.2 | --- | --- | -0.01(-0.05) | -5.41(-5.46) |
| 3,286.2 | 10,781.4 | -1.53 | -12.00 | -0.17 | -6.36 |
| 3,287.3 | 10,785.2 | -1.06 | -10.28 | -0.19 | -5.91 |
| 3,289.2 | 10,791.3 | -1.74 | -12.77 | -0.48 | -6.78 |
| 3,292.0 | 10,800.6 | -2.12 | -14.70 | -0.36 | -7.01 |
| | | **Lower unit** | | | |
| 3,410.4 | 11,189.0 | -1.58 | -10.66 | -0.73 | -6.56 |
| 3,412.9 | 11,197.3 | -2.66 | -11.26 | -2.23 | -9.09 |
| *3,413.3 | 11,198.4 | --- | --- | -3.53 | -11.40 |
| 3,417.1 | 11,211.0 | --- | --- | -1.71 | -8.54 |
| *3,418.6 | 11,215.7 | -3.15 | -12.46 | -2.61 | -10.66 |
| *3,418.8 | 11,216.5 | -3.25(-3.33) | -13.36(-13.13) | -2.95 | -11.71 |
| 3,419.0 | 11,217.3 | -1.35(-1.19) | -10.34 (-9.99) | -0.60 | -7.01 |
| 3,420.3 | 11,221.5 | -1.42 | -9.83 | +0.24 | -4.33 |
| 3,421.8 | 11,226.5 | -0.99 | -10.37 | -1.06 | -7.85 |

derived locally from dissolved marine carbonate grains that originated within individual sandstone beds or interbedded shales. The significantly lighter carbon compositions of dolomite in the upper part of the upper unit reflect precipitation from pore waters containing a component of light carbon possibly of organic origin and similar in composition to the fluids that precipitated calcite.

### Oxygen Isotopes

Variations in oxygen isotope compositions of calcite (-9.83 to -14.70 per mil) may reflect either changes in temperature with increasing burial depth or the influence of meteoric water circulating through the sandstones. Some of the isotopically light oxygen may be the result of carbonate precipitation at high temperatures while the rocks were close to maximum burial depth; however, $\delta^{18}O$ compositions of the cements do not consistently decrease with increasing burial depth, as would be expected if they formed at higher temperatures under conditions of deeper burial. Moreover, textural characteristics suggest that much of the calcite formed at relatively shallow burial depths. The differences in the depleted oxygen isotope compositions between the different units therefore most likely represent changes in the isotopic composition of meteoric waters during carbonate precipitation and, hence, record the isotopic evolution of these fluids through time.

The oxygen isotope compositions for dolomite are significantly lighter in the upper part of the upper unit than in the underlying sequences. This isotopically light oxygen probably was generated during diagenesis,

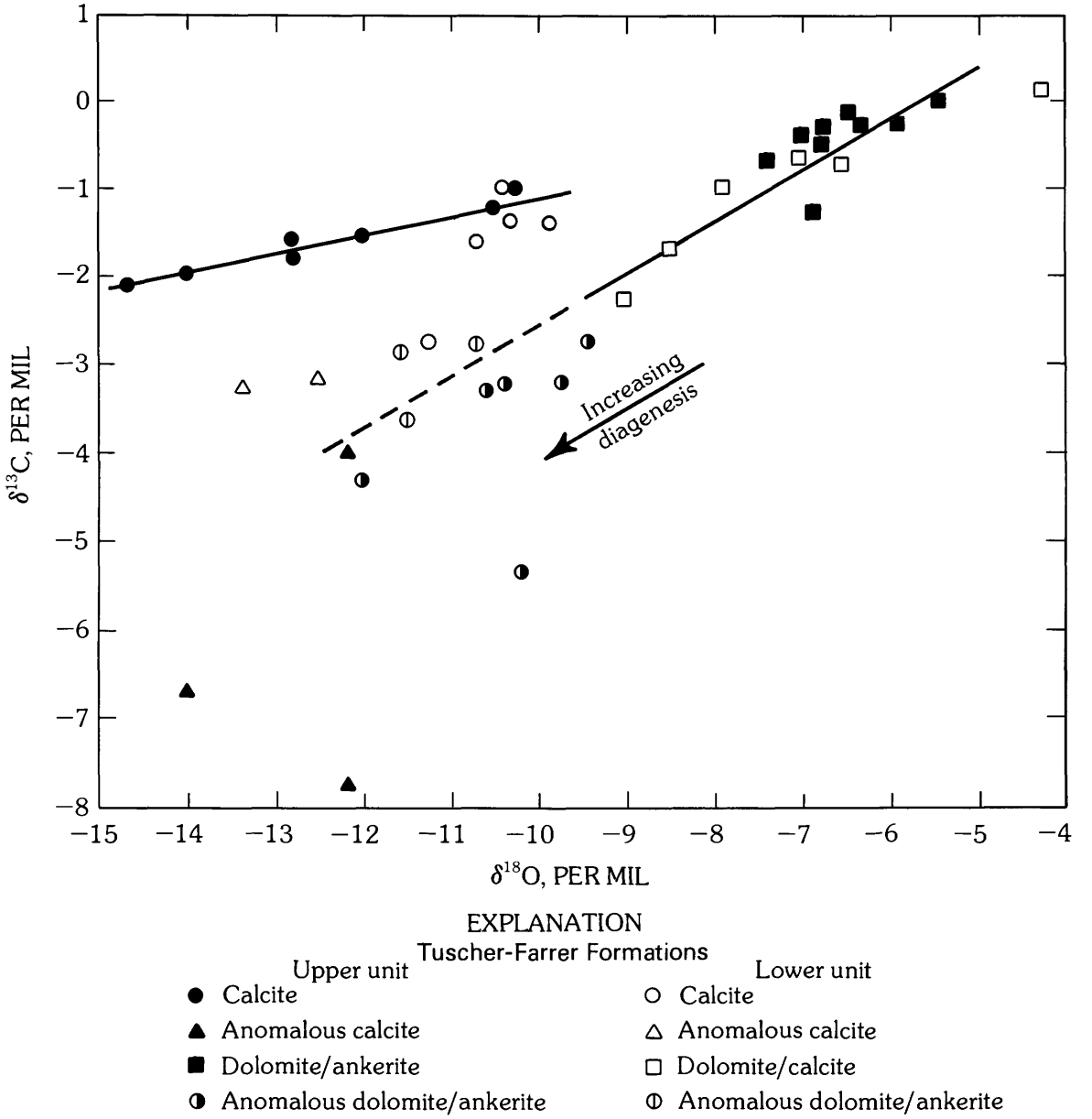


**Figure 11.** Carbon and oxygen isotope compositions for carbonate minerals in the undifferentiated Tuscher and Farrer Formations.

possibly from pore fluids having isotope compositions similar to the fluids that deposited calcite. Isotopically light calcite and dolomite may thus have formed during closely spaced diagenetic events.

### Sulfate Minerals

Textural relations between anhydrite, barite, and iron carbonate in the upper part of the upper unit in the undifferentiated Tuscher and Farrer Formations indicate that sulfate minerals formed relatively late in the burial history, following the generation of carbonate. The apparent association between sulfate mineral phases and bitumen suggests that sulfate-enriched pore waters associated with the maturation of organic matter may have played a role in the formation of anhydrite and barite. The chemical conditions governing the local dissolution of these minerals are uncertain.

### Authigenic Clay Mineral Formation

The complex authigenic clay mineral assemblage that characterizes Tuscher and Farrer sandstones in the Wilkin Ridge well reflects the evolution of fluid

chemistries during burial. Iron chlorite was the earliest authigenic mineral to form in the feldspathic sandstones after initial grain compaction. The absence of features indicative of widespread compaction in sandstones containing abundant chlorite is attributed to early formation of isopachous rim cement, as well as to development of carbonate that prevented further grain compaction. The rare occurrence of chlorite at grain contacts suggests that chlorite was not present as surface coatings on grains before the grains were reworked from the source area to the present site of deposition. Quartz overgrowths typically are poorly developed in sandstones that display widespread chlorite rim cement. Pittman and Lumsden (1968) have suggested that the growth of secondary quartz is limited in sandstones in which authigenic chlorite is abundant because nucleation sites for its growth commonly are not available. Chlorite cementation may have predated framework grain dissolution, as suggested by isopachous chlorite that commonly surrounds primary and secondary pores. The absence of numerous broken or crushed rims around the secondary pores implies that leaching of the host grain occurred after significant burial. Authigenic iron chlorite in the Tuscher and Farrer Formations may have been derived from volcanic grains, from the alteration of ferromagnesian minerals in preexisting lithic grains, from detrital clays of similar mineral composition, or from constituents in adjacent shale beds.

Discrete illite was one of the last mineral phases to precipitate in the Tuscher and Farrer sandstones. The presence of illite in secondary pores suggests that the illite formed when the rocks were near their maximum burial depth, either after or coincident with dissolution of ferroan calcite and anhydrite. The occurrence of illite also may be related to the transformation of smectite to illite. Most of the silica and aluminum necessary for illite crystallization probably was derived from nearby shales and transported into the more porous and permeable sandstone beds.

### Organic Matter

Small amounts of bitumen are present locally in the lower unit and in the upper part of the upper unit of the Tuscher and Farrer Formations. In some sandstones, the bitumen is along stylolites in areas where some dissolution of framework grains may have occurred. In other sandstones, the bitumen forms patches in clay-filled dissolution pores. Both the replacement of feldspar grains by iron carbonate and its subsequent enclosure by bitumen and the absence of bitumen inclusions in authigenic mineral cements suggest that most of this organic material formed relatively late in the burial history, after precipitation and subsequent dissolution of the authigenic minerals.

## RESERVOIR POTENTIAL

Reservoir property data for cored sandstones in the Wilkin Ridge well are presented in table 3. Measured porosity in the potential reservoir rocks is variable, ranging from 1.0 to 8.0 percent. Permeability is typically low, less than 0.1 millidarcy (mD), except in the upper part of the upper unit where it varies from 0.8 to 1.6 mD. Sandstone porosity and permeability generally decrease with increasing burial depth because of variations in mineral composition and grain size; higher porosity and permeability in the upper part of the upper unit probably correspond to the presence of bitumen. Coarser grained, better sorted sandstones commonly have higher porosity and permeability than do finer grained, more poorly sorted sandstones.

Porosity in the Tuscher and Farrer Formations is lowest in sandstones containing abundant detrital- and pseudo-matrix, ductile framework grains, widespread secondary quartz cement, and early-formed carbonate. It is enhanced in sandstones in which carbonate cement and chemically unstable grains such as feldspar and chert have been dissolved. Porosity in sandstones exhibiting early iron chlorite rim cement commonly is well developed; the early development of chlorite may have prevented further grain compaction and preserved initial pore volume for infilling by later mineral cements.

Low permeability is a characteristic of Upper Cretaceous nonmarine sandstones and can be attributed to the presence of detrital- and pseudo-matrix and mechanically unstable lithic fragments and to the development of authigenic clay minerals in secondary pores. Sandstones having these characteristics typically have a complex pore network and a high, irreducible water saturation resulting from the large surface areas of individual clay particles. As a consequence of reduced movement of fluids through the pore system, effective permeability is low.

## SOURCE ROCK EVALUATION

Selected samples of carbonaceous mudstone (shale) and coal from the Tuscher and Farrer Formations in the Wilkin Ridge well were evaluated geochemically by Rock-Eval pyrolysis and by vitrinite reflectance to determine their source rock characteristics and level of thermal maturity (tables 4, 5).

Tissot and Welte (1978) have indicated that clastic rocks having good source potential contain greater than 1 percent total organic carbon; the organic content of all samples from the undifferentiated Tuscher and Farrer Formations is greater than 1.0 percent.

Hydrocarbon and oxygen indices (table 4) are shown in a modified van Krevelen diagram (fig. 12). McIver (1967) and others have shown that the elemental

**Table 3.** Reservoir properties of sandstones in the undifferentiated Tuscher and Farrer Formations, Wilkin Ridge well

[Data provided by Exxon Oil Corporation (written commun., 1984)]

| Depth (meters) | Depth (feet) | Permeability (millidarcys) | Porosity (percent) | Residual saturation Oil (percent pore space) | Residual saturation Water (percent pore space) |
|---|---|---|---|---|---|
| | | **Upper unit** | | | |
| 3,134.0–134.3 | 10,282–83 | 0.09 | 2.7 | 9.2 | 55.3 |
| 3,135.8–136.1 | 10,288–89 | .10 | 2.4 | 9.3 | 64.9 |
| 3,136.1–136.4 | 10,289–90 | .92 | 5.5 | 9.7 | 31.2 |
| 3,136.4–136.7 | 10,290–91 | .14 | 5.5 | 11.4 | 35.7 |
| 3,136.7–136.8 | 10,291–92 | .14 | 5.5 | 8.5 | 20.5 |
| 3,136.8–137.3 | 10,292–93 | .11 | 6.9 | 10.7 | 18.3 |
| 3,137.3–137.6 | 10,293–94 | .12 | 5.7 | 8.2 | 13.1 |
| 3,137.6–137.9 | 10,294–95 | .13 | 5.1 | 10.9 | 21.8 |
| 3,137.9–138.2 | 10,295–96 | .23 | 6.3 | 9.2 | 23.8 |
| 3,138.2–138.5 | 10,296–97 | 1.60 | 6.2 | 9.5 | 21.8 |
| 3,138.5–138.8 | 10,297–98 | 1.30 | 6.8 | 11.6 | 23.2 |
| 3,138.8–139.1 | 10,298–99 | .65 | 6.7 | 8.9 | 20.4 |
| 3,139.1–139.4 | 10,299–00 | 1.30 | 4.8 | 10.3 | 23.6 |
| 3,139.4–140.1 | 10,301–02 | .11 | 5.9 | 3.6 | 61.5 |
| 3,140.1–140.4 | 10,302–03 | .08 | 5.5 | 4.2 | 54.2 |
| 3,274.9 | 10,744.4 | .07 | 6.9 | 2.0 | 72.1 |
| 3,275.1 | 10,745.1 | .06 | 6.8 | 0 | 40.0 |
| 3,275.7 | 10,746.9 | .06 | 6.3 | 0 | 44.4 |
| 3,275.8 | 10,747.4 | .06 | 6.5 | 0 | 44.1 |
| 3,276.1 | 10,748.3 | .05 | 5.7 | 0 | 40.4 |
| 3,276.5 | 10,749.5 | .05 | 5.0 | 0 | 51.5 |
| 3,276.7 | 10,750.4 | .01 | 1.4 | 0 | 40.3 |
| 3,277.0 | 10,751.2 | .03 | 2.3 | 0 | 47.4 |
| 3,278.0 | 10,754.4 | .07 | 6.5 | 0 | 44.4 |
| 3,278.2 | 10,755.3 | .06 | 4.0 | 0 | 63.4 |
| 3,278.6 | 10,756.5 | .28 | 5.1 | 0 | 63.8 |
| 3,278.8 | 10,757.3 | .14 | 7.0 | 0 | 48.6 |
| 3,279.1 | 10,758.1 | .11 | 7.0 | 0 | 35.4 |
| 3,279.6 | 10,759.7 | .08 | 7.3 | 0 | 50.2 |
| 3,279.7 | 10,760.2 | .07 | 6.8 | 0 | 36.3 |
| 3,280.0 | 10,761.2 | .07 | 6.4 | 0 | 65.1 |
| 3,280.5 | 10,762.8 | .06 | 6.4 | 0 | 37.2 |
| 3,280.7 | 10,763.5 | .05 | 5.9 | 0 | 55.7 |
| 3,280.9 | 10,764.1 | .04 | 6.1 | 0 | 51.1 |
| 3,281.3 | 10,765.4 | .05 | 7.9 | 0 | 47.8 |
| 3,281.5 | 10,766.2 | .04 | 7.2 | 0 | 59.2 |
| 3,281.9 | 10,767.3 | .03 | 5.5 | 0 | 54.8 |
| 3,282.2 | 10,768.4 | .04 | 6.2 | 0 | 55.9 |
| 3,282.5 | 10,769.2 | .04 | 6.2 | 0 | 63.4 |
| 3,282.8 | 10,770.2 | .02 | 5.5 | 0 | 69.8 |
| 3,283.1 | 10,771.4 | .04 | 5.9 | 0 | 45.8 |
| 3,283.5 | 10,772.7 | .05 | 6.7 | 0 | 56.2 |
| 3,283.7 | 10,773.4 | .03 | 4.5 | 0 | 38.5 |
| 3,284.0 | 10,774.2 | .05 | 6.4 | 0 | 34.6 |
| 3,284.3 | 10,775.4 | .05 | 7.1 | 0 | 53.1 |

**Table 3.** Reservoir properties of sandstones, Wilkin Ridge well—Continued

| Depth (meters) | Depth (feet) | Permeability (millidarcys) | Porosity (percent) | Residual saturation Oil (percent pore space) | Water |
|---|---|---|---|---|---|
| | | **Upper unit—Continued** | | | |
| 3,284.8 | 10,776.8 | .07 | 7.1 | 0 | 51.3 |
| 3,285.0 | 10,777.5 | .05 | 6.8 | 0 | 32.9 |
| 3,285.2 | 10,778.3 | .05 | 6.6 | 0 | 47.5 |
| 3,285.5 | 10,779.3 | .05 | 6.5 | 0 | 42.3 |
| 3,285.9 | 10,780.4 | .08 | 6.9 | 0 | 42.6 |
| 3,286.2 | 10,781.4 | .03 | 4.9 | 0 | 53.0 |
| 3,286.4 | 10,782.1 | .10 | 6.8 | 0 | 50.2 |
| 3,286.9 | 10,783.7 | .05 | 7.0 | 1.2 | 39.0 |
| 3,287.2 | 10,784.7 | .06 | 7.1 | 0 | 59.6 |
| 3,287.3 | 10,785.2 | .04 | 6.3 | 0 | 45.0 |
| 3,287.7 | 10,786.4 | .05 | 6.2 | 0 | 49.5 |
| 3,287.9 | 10,787.1 | .08 | 7.7 | 0 | 66.5 |
| 3,288.4 | 10,788.7 | .15 | 8.0 | 0 | 34.7 |
| 3,288.6 | 10,789.4 | .05 | 7.1 | 0 | 47.8 |
| 3,288.9 | 10,790.2 | .06 | 7.3 | 0 | 41.1 |
| 3,289.2 | 10,791.3 | .07 | 6.9 | 0 | 38.0 |
| 3,289.7 | 10,792.8 | .07 | 6.6 | 1.4 | 35.7 |
| 3,289.8 | 10,793.4 | .07 | 7.3 | 0 | 41.3 |
| 3,290.1 | 10,794.3 | .09 | 6.9 | 1.3 | 40.6 |
| 3,290.4 | 10,795.4 | .06 | 6.7 | 0 | 47.2 |
| 3,290.7 | 10,796.3 | .04 | 3.3 | 0 | 51.2 |
| 3,291.2 | 10,797.8 | .03 | 5.7 | 0 | 58.7 |
| 3,291.4 | 10,798.4 | .04 | 6.1 | 1.9 | 53.5 |
| 3,291.7 | 10,799.4 | .03 | 5.5 | 0 | 62.0 |
| 3,292.0 | 10,800.6 | .03 | 4.7 | 0 | 59.6 |
| | | **Lower unit** | | | |
| 3,413.0 | 11,197.5 | 0.02 | 4.9 | 27.6 | 31.5 |
| 3,413.3 | 11,198.4 | .07 | 4.8 | 15.9 | 13.6 |
| 3,418.0 | 11,213.8 | .01 | 2.0 | 5.7 | 68.6 |
| 3,418.2 | 11,214.6 | .02 | 1.6 | 9.2 | 55.2 |
| 3,418.6 | 11,215.7 | .01 | 1.5 | 0 | 57.4 |
| 3,418.7 | 11,216.3 | .01 | 1.0 | 10.1 | 60.6 |
| 3,419.0 | 11,217.3 | .01 | 1.0 | 0 | 76.3 |
| 3,420.6 | 11,222.4 | .02 | 1.5 | 0 | 58.0 |
| 3,421.0 | 11,223.7 | .02 | 2.7 | 4.6 | 64.0 |
| 3,421.3 | 11,224.7 | .02 | 2.4 | 7.7 | 77.4 |

compositions of organic matter are directly related to these index values and plot along well-defined curves that merge at high levels of thermal maturity. The consistently low hydrogen and oxygen indices (<70 mg/g of rock and <6 mg/g of rock) that characterize the Tuscher and Farrer Formations signify that potential source rocks contain type III (humic rich) kerogen that has attained a high level of thermal maturity. The level of thermal alteration estimated from the production indices (as high as 0.40) and from pyrolysis temperatures (*Tmax* >452 °C) suggests that the interbedded organic-rich mudstone and shales have reached the main stage of gas generation.

Genetic potential, a qualitative estimate of hydrocarbon resource potential, ranges from 0.74 to 2.61 mg/g; values greater than 2 mg/g suggest good liquid hydrocarbon potential. Source beds in the Tuscher and Farrer are

**Table 4.** Geochemical and Rock-Eval pyrolysis data for potential source rocks in the undifferentiated Tuscher and Farrer Formations, Wilkin Ridge well

[Asterisk (*), sample from upper unit]

| Depth (meters) | Depth (feet) | Total organic carbon *TOC* (percent) | Extractable organic matter *EOM* (ppm) | Saturated hydrocarbons *SATS* (ppm) | Aromatic hydrocarbons *AROMS* (ppm) | *SATS/AROMS* | Asphaltines and polar organic compounds (ppm) | Extractable hydrocarbons *SATS+AROMS* (ppm) | Extractable hydrocarbons *HC/TOC* (mg/g of rock) |
|---|---|---|---|---|---|---|---|---|---|
| *3,134.0 | 10,282.0 | 1.35 | 238 | 53 | 101 | 0.52 | 84 | 154 | 11 |
| *3,143.1 | 10,312.0 | 1.76 | 569 | 186 | 261 | .71 | 122 | 447 | 25 |
| 3,409.5 | 11,186.0 | 2.02 | 386 | 171 | 123 | 1.33 | 92 | 294 | 15 |
| 3,410.4 | 11,189.0 | 1.10 | 484 | 309 | 94 | 3.29 | 81 | 403 | 37 |
| 3,414.1 | 11,201.0 | 2.35 | 760 | 413 | 188 | 2.20 | 159 | 601 | 26 |
| 3,416.5 | 11,209.0 | 2.34 | 831 | 507 | 195 | 2.60 | 129 | 702 | 30 |
| 3,420.3 | 11,221.5 | 1.43 | 360 | 105 | 153 | .69 | 102 | 258 | 18 |

| Depth (meters) | Depth (feet) | Free hydrocarbon $S_1$ (mg/g) | Pyrolyzable hydrocarbon $S_2$ (mg/g) | Organic $CO_2$ $S_3$ (mg/g) | Genetic potential $S_1+S_2$ (mg/g) | Production index $S_1/(S_1+S_2)$ | Hydrogen index $S_2/TOC$ (mg/g of rock) | Oxygen index $S_3/TOC$ (mg/g of rock) | Maximum temperature *Tmax* (°C) |
|---|---|---|---|---|---|---|---|---|---|
| *3,134.0 | 10,282.0 | 0.20 | 0.55 | 0.18 | 0.74 | 0.27 | 40 | 13 | 461 |
| *3,143.1 | 10,312.0 | .55 | 1.01 | .17 | 1.56 | .35 | 57 | 9 | 452 |
| 3,409.5 | 11,186.0 | .65 | 1.03 | .16 | 1.68 | .39 | 51 | 8 | 468 |
| 3,410.4 | 11,189.0 | .67 | .37 | .51 | 1.04 | .64 | 34 | 46 | 476 |
| 3,414.1 | 11,201.0 | .99 | 1.54 | .15 | 2.54 | .39 | 66 | 6 | 474 |
| 3,416.5 | 11,209.0 | 1.00 | 1.65 | .15 | 2.61 | .37 | 70 | 6 | 463 |
| 3,420.3 | 11,221.5 | .39 | .59 | .19 | .98 | .39 | 42 | 13 | 470 |

DEFINITIONS

| | |
|---|---|
| $S_1$ | Quantity of organic matter existing as free or adsorbed hydrocarbons |
| $S_2$ | Quantity of hydrocarbons and hydrocarbonlike compounds released from the sample at pyrolytic temperatures (250–550 °C) |
| $S_3$ | Quantity of $CO_2$ released at pyrolytic temperatures (>250–390 °C) |
| Genetic potential ($S_1+S_2$) | Sum of original genetic potential and residual genetic potential. A minimum value for oil source rocks is considered to be 2 mg/g |
| Production index ($S_1/(S_1+S_2)$) | Transformation ratio or index of maturation. With respect to hydrocarbon generation, the transition from immature to mature occurs at about 0.1 |
| Hydrogen index ($S_2/TOC$) | Quantity of hydrocarbons (measured as $S_2$) in the sample relative to organic carbon content |
| Oxygen index ($S_3/TOC$) | Quantity of $CO_2$ (measured as $S_3$) in the sample relative to organic carbon content |
| *Tmax* | Temperature at maximum hydrocarbon generation during pyrolysis ($S_2$) and an indicator of prior thermal history. The transition from immature to mature occurs at about 440 °C |

composed predominantly of nonmarine, terrestrially derived organic matter that contains condensed polyaromatic and oxygen-rich structures, and, as a result, most hydrocarbons generated in these units will be gas. Hydrocarbons in the lower unit (11,186 and 11,209 ft; 3,049.5–3,416.5 m) display a shift to higher saturate to aromatic ratios (*SATS/AROMS*>1; table 4) and pristane to phytane ratios (>4, table 5). This suggests either a possible source change or staining by migrated hydrocarbons. The higher ratios, as well as the relatively constant hydrogen indices for both the upper and lower units and the high production index for the sample at 11,189 ft (3,410.4 m), collectively suggest the rocks have been stained to differing degrees by migrated hydrocarbons.

Vitrinite reflectance values ($R_o$) for coaly samples from the Wilkin Ridge well vary widely: $R_o$ values for the lower unit at depths of about 11,000 ft (3,353 m) range from 0.88 to 1.32 percent, whereas $R_o$ values for the upper unit at burial depths of about 10,000 ft (3,048 m) range from 0.73 to 0.75 percent (table 5). These reflectance values are significantly higher than those reported by Pitman, Anders, and others (1986) and Pitman and others (1987) for the Neslen, Tuscher, and Farrer Formations at shallower burial depths in the eastern part of

**Table 5.** Vitrinite reflectance and gas chromatography analyses of potential source rocks in the undifferentiated Tuscher and Farrer Formations, Wilkin Ridge well
[Asterisk (*), weathered sample; N.S., no sample]

| Depth (meters) | Depth (feet) | Vitrinite reflectance ($R_o$, in pct.) | Pristane/ phytane ratio | $nC_{17}$ pristane ratio |
|---|---|---|---|---|
| 3,134.0 | 10,282.0 | 0.73 | 2.1 | 3.6 |
| 3,143.1 | 10,312.0 | .75 | 2.9 | 3.4 |
| *3,407.7 | 11,180.0 | 1.22 | N.S. | N.S. |
| 3,409.5 | 11,186.0 | .97 | 4.2 | 1.8 |
| 3,410.4 | 11,189.0 | 1.32 | 4.4 | 1.7 |
| *3,414.1 | 11,201.0 | .93 | 4.5 | 1.3 |
| 3,416.5 | 11,209.0 | .95 | 4.4 | 2.1 |
| 3,420.2 | 11,221.5 | .95 | 2.9 | 2.1 |
| 3,422.6 | 11,229.0 | .88 | N.S. | N.S. |

the basin. The reliability of these values is uncertain because of their extreme variability. The unusually high values may reflect either a component of altered vitrinite or possibly vitrinite reworked from older rock because there is no direct evidence to support either a late-stage heating event or migration of high-temperature fluids in the area of the well. Some values also may be lower than their true reflectance because of suppression effects resulting from abnormally high formation pressures (C.W. Spencer, oral commun., 1986). Despite variations in individual reflectance values, it is evident that the thermal maturity of these Cretaceous source rocks increases with depth of burial. In the more deeply buried Tuscher and Farrer rocks, gas-prone source rocks are well within the catagenesis zone of hydrocarbon generation, and these rocks probably have produced significant amounts of thermal gas.

## BURIAL AND THERMAL HISTORY

The hydrocarbon generation history of the undifferentiated Tuscher and Farrer Formations was evaluated by using Lopatin-style burial reconstruction, a method in which both time and temperature are taken into account to model sediment-burial and thermal history through geologic time. The depositional and tectonic history of Cretaceous rocks in the vicinity of the Wilkin Ridge well is shown by the Lopatin reconstruction of burial depth and temperature as a function of time for the Tuscher and Farrer Formations (fig. 13). The data used to construct the model (table 6) are from Larson and others (1975), Fouch and others (1983), and Hansen (1984). The burial history model assumes a uniform

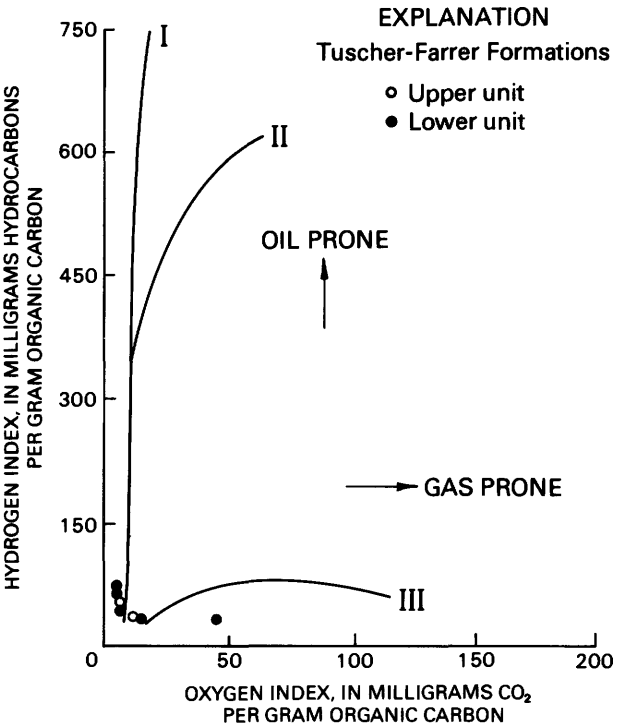


**Figure 12.** Modified van Krevelen diagram showing hydrogen and oxygen indices for humic-rich source rocks in the undifferentiated Tuscher and Farrer Formations, Wilkin Ridge well. Roman numerals indicate kerogen types I, II, and III.

sedimentation rate and a constant geothermal gradient with depth. The present-day geothermal gradient in the vicinity of the Wilkin Ridge well is estimated to be the same as the gradient in the Natural Buttes area, that is, 1.6 °F/100 ft (29 °C/km) (Chapman and others, 1984). This gradient is similar to gradients calculated from drill-stem test results for wells near the Wilkin Ridge well (D.E. Anders, unpub. data, 1986) and is within the range reported for sedimentary basins in the Rocky Mountain region. The paleogeothermal gradient in the model is considered to be the same as the present-day gradient; any differences probably amount to no more than a few degrees.

Waples (1980) demonstrated that the time-temperature index (*TTI*), the length of time sediment has been exposed to a specific paleotemperature interval, can be used as a maturation indicator in a Lopatin model because it correlates well with other commonly used parameters such as vitrinite reflectance. In our study, vitrinite reflectance, as inferred from *TTI* for the top of the Neslen, was systematically compared with measured reflectance values for the same unit in order to constrain the timing and magnitude of tectonic and associated erosional events and the variations in the geothermal gradient through time. Based on *TTI*, the best-fit time-temperature model (fig. 13) indicates that sedimentary

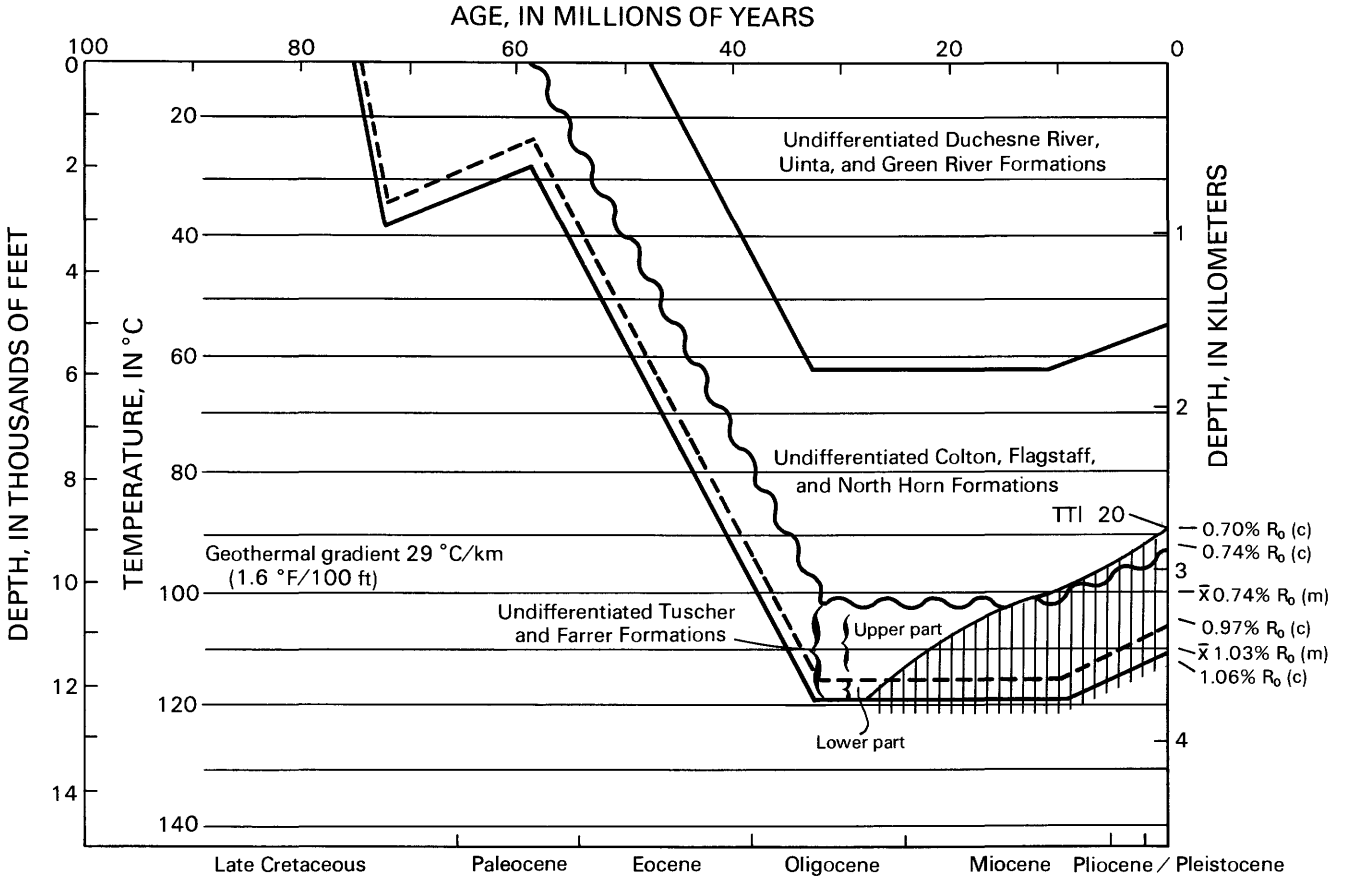


**Figure 13.** Modified time-temperature Lopatin diagram showing reconstructed burial and thermal history for Cretaceous and Tertiary rocks in the area of the Wilkin Ridge well. Isotherms reflect past and present geothermal gradients; wavy line represents Cretaceous–Tertiary boundary. Hachured area, zone of active hydrocarbon generation ($R_o$ >0.07 percent; c, calculated $R_o$ value; m, measured $R_o$ value.

burial through tectonic subsidence controlled the maturation of organic matter in Cretaceous rocks in the central part of the Uinta basin. Moreover, fluctuations in the geothermal gradient do not appear to be an important influence governing the maturation of hydrocarbons.

Regional studies in the Uinta basin indicate that relatively continuous sedimentation in marine and continental depositional environments during the Cretaceous was followed by a complex depositional history during the Cenozoic. A change in deformation style from Sevier thrusting to Laramide basement-controlled deformation, beginning in the Late Cretaceous and continuing through the Paleogene (Fouch and others, 1983; Lawton, 1983), was accompanied by rapid sedimentation throughout the basin as it tectonically subsided. By the middle Oligocene, the Tuscher and Farrer Formations had attained their maximum burial depth following deposition of more than 9,000 feet (2,743 m) of Tertiary sediments. Between the early Oligocene and the present, the depositional and tectonic history is uncertain because rocks that span this time period are not preserved in the basin. From the late Miocene (about 10 Ma) to the present, regional uplift and erosion associated with the development of the Colorado Plateau were widespread through the Rocky Mountain region (Larson and others, 1975; Hansen, 1984). During the early Oligocene, post-Laramide uplift and erosion associated with the development of the Gilbert Peak erosion surface may have extended southward into the central part of the Uinta basin (W.R. Hansen, oral commun., 1986). If this was the case, erosion during this period probably was minor in comparison with erosion during plateau uplift and did not affect the hydrocarbon generation history.

Based on a present-day temperature gradient of 1.6 °F/100 ft (29 °C/km), the Lopatin model (fig. 13) indicates that about 1,000 feet (305 m) of Tertiary strata may have been eroded from the area of the Wilkin Ridge well from the late Miocene to the present. In the Indian Canyon area, about 30 miles northwest of the well, a minimum of 2,000 ft (610 m) of upper Eocene lacustrine deposits lies stratigraphically above the present erosion surface in the Wilkin Ridge area (Ray and others, 1956);

**Table 6.** Parameters used to reconstruct the burial and tectonic history in the area of the Wilkin Ridge well

[N.A., not applicable; query (?), date uncertain. Data from Larson and others (1975), Fouch and others (1983), and Hansen (1984)]

| Depositional or tectonic event | Time (Ma) | Formation boundaries (depth, in ft) | Thickness (feet) | Cumulative thickness (feet) |
|---|---|---|---|---|
| Colorado Plateau uplift and erosion ... | 0 | 0- 5,090 | -800 | 11,242 |
| Depositional hiatus ..... | 10 | N.A. | 0 | 12,042 |
| Undifferentiated Duchesne River, Uinta, and Green River Formations ..... | 32 | 0- 5,090 | 5,890 | 12,042 |
| Colton, Flagstaff, and North Horn Formations ..... | 47 | 5,090- 9,555 | 4,465 | 6,152 |
| Cretaceous-Tertiary boundary erosion ..... | 58 | 9,555 | -1,500 | 1,687 |
| Undifferentiated Tuscher and Farrer Formations. | | | | |
| Upper part ..... | 72 | 9,555-11,090 | 2,735 | 3,187 |
| Lower part ..... | 74? | 11,090-11,542 | 452 | 452 |
| Bluecastle Tongue of the Castlegate Sandstone ..... | 75 | 11,542-12,140 | 598 | N.A. |

an equally thick lacustrine and alluvial sequence should have been deposited contemporaneously in the Wilkin Ridge area. If a geothermal gradient of 1.4 °F/100 ft (27 °C/km) is used in the Lopatin model instead of 1.6 °F/100 ft (29 °C/km), then 2,000 ft (610 m) of erosion is compatible with measured vitrinite values. There is no evidence to suggest that the paleogeothermal gradient was lower than the present gradient, thus it is possible that the few measured vitrinite values we could obtain for this study do not accurately reflect the thermal history. Additional vitrinite data throughout the entire section would resolve this uncertainty and support more confident estimates of the paleogeothermal gradient.

It is evident from the burial history model that potential source rocks in the Tuscher and Farrer Formations in the area of Wilkin Ridge were immature until they reached maximum burial depths during the early Oligocene, at which time they attained their present thermal maturity. Although the duration of maximum burial for these Cretaceous rocks was brief, about 20 million years, hydrocarbon generation was most active during this period. If significant hydrocarbon generation is assumed to begin at a vitrinite reflectance of about 0.7 percent (*TTI* 20; Waples, 1980), then active hydrocarbon generation in potential source beds in the Tuscher and Farrer Formations occurred between approximately 10 and 30 Ma when the rocks were close to maximum burial (about 10,500–12,000 ft, 3,200–3,658 m). Based on the Lopatin time-temperature model, paleotemperatures during maximum burial of the Tuscher and Farrer Formations are estimated to have been as high as 248 °F (120 °C); however, the time-independent relationship of Barker and Pawlewicz (1986) indicates that maximum paleotemperatures for the Tuscher and Farrer exceeded 300 °F (150 °C). These temperatures seem unlikely, inasmuch as they require a much higher paleogeothermal gradient and one inconsistent with the reconstructed burial history of the central part of the basin. The rate of hydrocarbon generation in the Tuscher and Farrer Formations may have declined from 10 Ma to the present because of the removal of overburden during Colorado Plateau uplift. *TTI* calculations indicate that a vitrinite reflectance level of about 0.70 percent (*TTI* 20) projects to a present-day burial depth of about 9,000 ft (2,743 m), a depth that closely approximates the depth of the Cretaceous-Tertiary boundary. Thus, the Tuscher and Farrer rocks as well as older rocks are still undergoing hydrocarbon generation assuming they contain sufficient quantities of organic matter.

Spencer (1987) and Law (1984) have suggested that

generation of hydrocarbons in low-permeability reservoir rocks in the Rocky Mountain region contributed to the development of high formation pressures. Indirect pressure data for the Wilkin Ridge well (bottom-hole temperatures and mud weights) indicate that the lower cored sequence in the undifferentiated Tuscher and Farrer Formations currently is overpressured. Such an overpressured system may have created some of the local occurrences of closed hairline fractures in sandstones and shale beds in both the lower and upper units; similar fractures have been reported in rocks of similar age and origin from other parts of the basin (Pitman, Anders, and others, 1986; Pitman and others, 1987). It is also plausible that abnormally high pressures existed in younger rocks when they were at maximum burial and undergoing active hydrocarbon generation. As a result of uplift and erosion during the late Tertiary, these higher pressures may have dissipated to form the lower pressure regime that now characterizes the basin.

## REFERENCES CITED


Barker, C.E., and Pawlewicz, M.J., 1986, The correlation of vitrinite reflectance with maximum temperature in humic organic matter, *in* Buntebarth, Gunter, and Stegena, L., eds., Lecture notes in earth sciences, v. 5; paleogeothermics: New York, Springer-Verlag, p. 79–93.

Chapman, D.S., Keho, T.H., Bauer, M.S., and Picard, M.D., 1984, Heat flow in the Uinta Basin determined from bottom hole temperature (BHT) data: Geophysics, v. 49, p. 453–466.

Dickinson, W.R., Lawton, T.F., and Inman, K.F., 1986, Sandstone detrital modes, central Utah foreland region; stratigraphic record of Cretaceous–Paleogene tectonic evolution: Journal of Sedimentary Petrology, v. 56, p. 276–293.

Fisher, D.J., Erdmann, C.E., and Reeside, J.B., Jr., 1960, Cretaceous and Tertiary formations of the Book Cliffs, Carbon, Emery, and Grand Counties, Utah, and Garfield and Mesa Counties, Colorado: U.S. Geological Survey Professional Paper 332, 80 p.

Folk, R.L., 1974, Petrology of sedimentary rocks: Austin, Texas, Hemphill's, 182 p.

Fouch, T.D., Lawton, T.F., Nichols, D.J., Cashion, W.B., and Cobban, W.A., 1983, Patterns and timing of synorogenic sedimentation in Upper Cretaceous rocks of central and northeast Utah, *in* Reynolds, M.W., and Dolly, E.D., eds., Mesozoic paleogeography of the west-central United States: Society of Economic Paleontologists and Mineralogists, Rocky Mountain Section, Rocky Mountain Paleogeography Symposium, 2nd, Denver, 1983, p. 305–336.

Gross, M.G., 1964, Variations in the $O^{18}/O^{16}$ and $C^{13}/C^{12}$ ratios of diagenetically altered limestones in the Bermuda Islands: Journal of Geology, v. 72, no. 2, p. 170–194.

Hansen, W.R., 1984, Post-Laramide tectonic history of the eastern Uinta Mountains, Utah, Colorado, and Wyoming: The Mountain Geologist, v. 21, no. 1, p. 5–29.

Keighin, C.W., and Fouch, T.D., 1981, Depositional environments and diagenesis of some nonmarine Upper Cretaceous reservoir rocks, Uinta basin, Utah, *in* Ethridge, F.G., and Flores, R.M., eds., Recent and ancient nonmarine depositional environments; models for exploration: Society of Economic Paleontologists and Mineralogists Special Publication 31, p. 109–125.

Larson, E.E., Osima, M., and Bradley, W.C., 1975, Late Cenozoic basic volcanism in northwestern Colorado and its implications concerning tectonism and the origin of the Colorado River system, *in* Curtis, B.F., ed., Cenozoic history of the southern Rocky Mountains: Geological Society of America Memoir 144, p. 155–178.

Law, B.E., 1984, Relationships of source-rock, thermal maturity, and overpressuring to gas generation and occurrence in low-permeability Upper Cretaceous and lower Tertiary rocks, greater Green River basin, Wyoming, Colorado and Utah, *in* Woodward, Jane, Meissner, F.F., and Clayton, J.L., eds., Symposium on hydrocarbon source rocks of the greater Rocky Mountain region: Rocky Mountain Association of Geologists Symposium, Denver, 1984, p. 469–490.

Lawton, T.F., 1983, Late Cretaceous fluvial systems and the age of foreland uplifts in central Utah, *in* Lowell, J.D. and Gries, Robbie, eds., Rocky Mountain foreland basins and uplifts: Rocky Mountain Association of Geologists Field Conference, Steamboat Springs, Colorado, 1983, p. 181–199.

McIver, R.D., 1967, Composition of kerogen-clue to its role in the origin of petroleum, *in* Origin of oil, geology, and geophysics: World Petroleum Congress, 7th, Mexico, 1967, Proceedings, v. 2: London, Elsevier, p. 25–36.

Osterwald, F.W., Maberry, J.O., and Dunrud, C.R., 1974, Bedrock, surficial and economic geology of the Sunnyside coal mining district, Carbon and Emery Counties, Utah: U.S. Geological Survey Professional Paper 1166, 68 p.

Pitman, J.K., Anders, D.E., Fouch, T.D., and Nichols, D.J., 1986, Hydrocarbon potential of nonmarine Upper Cretaceous and lower Tertiary rocks, eastern Uinta basin, Utah, *in* Spencer, C.W., and Mast, R.F., eds., Geology of tight gas reservoirs: American Association of Petroleum Geologists Studies in Geology 24, p. 235–252.

Pitman, J.K., Franczyk, K.J., and Anders, D.E., 1987, Marine and nonmarine gas-bearing rocks in the Upper Cretaceous Blackhawk and Neslen Formations, eastern Uinta basin, Utah; sedimentology, diagenesis, and source-rock potential: American Association of Petroleum Geologists Bulletin, v. 71, no. 1, p. 76–94.

Pitman, J.K., Goldhaber, M.B., and Fouch, T.D., 1986, Mineralogy and stable isotope geochemistry of carbonate and sulfate minerals in diagenetically altered Tertiary and Cretaceous sandstones, Uinta basin, Utah, *in* Mumpton, F.A., ed., Studies in diagenesis: U.S. Geological Survey Bulletin 1578, p. 207–218.

Pittman, E.D., and Lumsden, D.N., 1968, Relationship between chlorite coatings on quartz grains and porosity, Spiro Sand, Oklahoma: Journal of Sedimentary Petrology, v. 38, p. 668–670.

Price, L.C., 1983, Geologic time as a parameter in organic metamorphism and vitrinite reflectance as an absolute paleogeothermometer: Journal of Petroleum Geology, v. 6, p. 5–38.

Ray, R.G., Kent, B.H., and Dane, C.H., 1956, Stratigraphy and photogeology of the southwestern part of Uinta basin, Duchesne and Uintah Counties, Utah: U.S. Geological Survey Oil and Gas Investigations Map OM-171, 2 sheets, scale 1:63,360.

Siebert, R. M., 1984, A theory of framework grain dissolution in sandstones, *in* McDonald, D.A., and Surdam, R.C., eds., Clastic diagenesis: American Association of Petroleum Geologists Memoir 37, p. 163–175.

Spencer, C.W., 1987, Hydrocarbon generation as a mechanism for overpressuring in the Rocky Mountain region: American Association of Petroleum Geologists Bulletin, v. 71, no. 4, p. 368–388.

Tissot, B.P., and Welte, D.H., 1978, Petroleum formation and occurrence; a new approach to oil and gas exploration: New York, Springer-Verlag, 538 p.

Waples, D.W., 1980, Time and temperature in petroleum formation; application of Lopatin's method to petroleum exploration: American Association of Petroleum Geologists Bulletin, v. 64, no. 6, p. 916–926.

Weber, J.N., 1964, Trace element composition of dolostones and dolomites and its bearing on the dolomite problem: Geochimica et Cosmochimica Acta, v. 28, no. 11, p. 1817–1868.



☆ U.S. GOVERNMENT PRINTING OFFICE:1988—575-382